

Diagrammatic perturbation theory and the pseudogap

P. Monthoux

Cavendish Laboratory, University of Cambridge

Madingley Road, Cambridge CB3 0HE, United Kingdom

(February 18, 2019)

Abstract

We study a model of quasiparticles on a two-dimensional square lattice coupled to Gaussian distributed dynamical molecular fields. We consider two types of such fields, a vector molecular field that couples to the quasiparticle spin-density and a scalar field coupled to the quasiparticle number density. The model describes quasiparticles coupled to spin or charge fluctuations, and is solved by a Monte Carlo sampling of the molecular field distributions. The nonperturbative solution is compared to various approximations based on diagrammatic perturbation theory. When the molecular field correlations are sufficiently weak, the diagrammatic calculations capture the qualitative aspects of the quasiparticle spectrum. For a range of model parameters near the magnetic boundary, we find that the quasiparticle spectrum is qualitatively different from that of a Fermi liquid, in that it shows a double peak structure, and that the diagrammatic approximations we consider fail to reproduce, even qualitatively, the nonperturbative results of the Monte Carlo calculations. This suggests that the magnetic pseudogap induced by a coupling to antiferromagnetic spin-fluctuations and the spin-splitting of the quasiparticle peak induced by a coupling to ferromagnetic spin-fluctuations lie beyond diagrammatic perturbation theory. While a pseudogap opens when quasi-

particles are coupled to antiferromagnetic fluctuations, such a pseudogap is not observed in the corresponding charge-fluctuation case for the range of parameters studied, where vertex corrections are found to effectively reduce the strength of the interaction. This suggests that one has to be closer to the border of long-range order to observe pseudogap effects in the charge-fluctuation case than for a spin-fluctuation induced interaction under otherwise similar conditions. The diagrammatic approximations that contain first order vertex corrections show the enhancement of the spin-fluctuation induced interaction and the suppression of the effective interaction in the charge-fluctuation case. However, for the range of model parameters considered here, the multiple spin or charge-fluctuation exchange processes not included in the diagrammatic approximations considered are found to be important, especially for quasiparticles coupled to charge fluctuations.

PACS Nos. 71.27.+a

I. INTRODUCTION

The concept of elementary excitations and the diagrammatic perturbation-theoretic methods borrowed from quantum field theory have given us, over the past decades, many powerful insights into the behavior of materials. In a number of cases, however, these concepts and methods don't seem to work. In previous papers [1,2], we presented results on a nonperturbative extension of the magnetic interaction model, which had until then been extensively used in the context of diagrammatic approaches. These latter applications were successful in many respects: in the Eliashberg approximation, the magnetic interaction model correctly anticipated the pairing symmetry of the Cooper state in the copper oxide superconductors [3] and is consistent with spin-triplet p-wave pairing in superfluid 3He [for a recent review see, e.g., ref. [4]]. One also gets the correct order of magnitude of the superconducting and superfluid transition temperature T_c when the model parameters are inferred from experiments in the normal state of the above systems. However, in Ref. [1] it was found that when the model was treated nonperturbatively and one approached the border of magnetic long-range order, the quasiparticle spectrum showed qualitative changes not captured by the Eliashberg approximation. In Ref. [1], we raised the possibility that these qualitative changes, namely the opening of a pseudogap in the quasiparticle spectrum, were intrinsically nonperturbative in nature. In this paper, we examine this possibility by comparing the nonperturbative results to various kinds of perturbation-theoretic approximations.

The paper is organized as follows. In the next section we describe the model as well as the various perturbation-theoretic approximations to be compared to the Monte Carlo calculations. Section III contains the results of the nonperturbative and diagrammatic calculations. Section IV contains a discussion of the results and finally we give a summary and outlook

II. MODEL

The model and its motivation have been extensively discussed in Ref. [1]. Here we only give the definitions relevant to the present discussion. We consider particles on a two-dimensional square lattice whose Hamiltonian in the absence of interactions is

$$\hat{h}_0(\tau) = - \sum_{i,j,\alpha} t_{ij} \psi_{i\alpha}^\dagger(\tau) \psi_{j\alpha}(\tau) - \mu \sum_{i\alpha} \psi_{i\alpha}^\dagger(\tau) \psi_{i\alpha}(\tau) \quad (2.1)$$

where t_{ij} is the tight-binding hopping matrix, μ the chemical potential and $\psi_{i\alpha}^\dagger$, $\psi_{i\alpha}$ respectively create and annihilate a fermion of spin orientation α at site i . We take $t_{ij} = t$ if sites i and j are nearest neighbors and $t_{ij} = t'$ if sites i and j are next-nearest neighbors.

To introduce interactions between the particles, we couple them to a dynamical molecular (or Hubbard-Stratonovich) field. It is instructive to consider two different types of molecular fields. In the first instance, we consider a vector Hubbard-Stratonovich field that couples locally to the fermion spin density. We also consider the case of a scalar field that couples locally to the fermion number density. This case corresponds to a coupling to charge-fluctuations or, within the approximation we are using here, "Ising"-like magnetic fluctuations where only longitudinal modes are present. The Hamiltonians at imaginary time τ for particles coupled to the fluctuating exchange or scalar dynamical field are then

$$\hat{h}(\tau) = \hat{h}_0(\tau) - \frac{g}{\sqrt{3}} \sum_{i\alpha\gamma} \mathbf{M}_i(\tau) \cdot \psi_{i\alpha}^\dagger(\tau) \sigma_{\alpha\gamma} \psi_{i\gamma}(\tau) \quad (2.2)$$

$$\hat{h}(\tau) = \hat{h}_0(\tau) - g \sum_{i\alpha} \Phi_i(\tau) \psi_{i\alpha}^\dagger(\tau) \psi_{i\alpha}(\tau) \quad (2.3)$$

where $\mathbf{M}_i(\tau) = (M_i^x(\tau), M_i^y(\tau), M_i^z(\tau))^T$ and $\Phi_i(\tau)$ are the real vector exchange and scalar Hubbard-Stratonovich fields respectively, and g the coupling constant. The reason for the choice of an extra factor $1/\sqrt{3}$ in Eq. (2.2) becomes clear later.

Since we ignore the self-interactions of the molecular fields, their distribution is Gaussian and given by [2,1]

$$\mathcal{P}[\mathbf{M}] = \frac{1}{Z} \exp \left(- \sum_{\mathbf{q}, \nu_n} \frac{\mathbf{M}(\mathbf{q}, i\nu_n) \cdot \mathbf{M}(-\mathbf{q}, -i\nu_n)}{2\alpha(\mathbf{q}, i\nu_n)} \right) \quad (2.4)$$

$$Z = \int D\mathbf{M} \exp \left(- \sum_{\mathbf{q}, \nu_n} \frac{\mathbf{M}(\mathbf{q}, i\nu_n) \cdot \mathbf{M}(-\mathbf{q}, -i\nu_n)}{2\alpha(\mathbf{q}, i\nu_n)} \right) \quad (2.5)$$

in the case of a vector exchange molecular field and

$$\mathcal{P}[\Phi] = \frac{1}{Z} \exp \left(- \sum_{\mathbf{q}, \nu_n} \frac{\Phi(\mathbf{q}, i\nu_n) \Phi(-\mathbf{q}, -i\nu_n)}{2\alpha(\mathbf{q}, i\nu_n)} \right) \quad (2.6)$$

$$Z = \int D\Phi \exp \left(- \sum_{\mathbf{q}, \nu_n} \frac{\Phi(\mathbf{q}, i\nu_n) \Phi(-\mathbf{q}, -i\nu_n)}{2\alpha(\mathbf{q}, i\nu_n)} \right) \quad (2.7)$$

in the case of a scalar Hubbard-Stratonovich field. In both cases $\nu_n = 2\pi nT$ since the dynamical molecular fields are periodic functions in the interval $[0, \beta = 1/T]$. The Fourier transforms of the molecular fields are defined as

$$\mathbf{M}_{\mathbf{R}}(\tau) = \sum_{\mathbf{q}, \nu_n} \mathbf{M}(\mathbf{q}, i\nu_n) \exp \left(- i[\mathbf{q} \cdot \mathbf{R} - \nu_n \tau] \right) \quad (2.8)$$

$$\Phi_{\mathbf{R}}(\tau) = \sum_{\mathbf{q}, \nu_n} \Phi(\mathbf{q}, i\nu_n) \exp \left(- i[\mathbf{q} \cdot \mathbf{R} - \nu_n \tau] \right) \quad (2.9)$$

We consider the case where there is no long-range magnetic or charge order. The average of the dynamical molecular fields must then vanish and their Gaussian distributions Eqs. (2.4,2.6) are completely determined by their variance $\alpha(\mathbf{q}, i\nu_n)$, which we take to be

$$\alpha(\mathbf{q}, i\nu_n) = \begin{cases} \frac{1}{2} \frac{T}{N} \chi(\mathbf{q}, i\nu_n) & \text{if } \mathbf{M}(\mathbf{q}, i\nu_n) \text{ or } \Phi(\mathbf{q}, i\nu_n) \text{ complex} \\ \frac{T}{N} \chi(\mathbf{q}, i\nu_n) & \text{if } \mathbf{M}(\mathbf{q}, i\nu_n) \text{ or } \Phi(\mathbf{q}, i\nu_n) \text{ real} \end{cases} \quad (2.10)$$

where N is the number of allowed wavevectors in the Brillouin zone. Then

$$\langle M_i(\mathbf{q}, i\nu_n) M_j(\mathbf{k}, i\Omega_n) \rangle = \frac{T}{N} \chi(\mathbf{q}, i\nu_n) \delta_{\mathbf{q}, -\mathbf{k}} \delta_{\nu_n, -\Omega_n} \delta_{i,j} \quad (2.11)$$

$$\langle \Phi(\mathbf{q}, i\nu_n) \Phi(\mathbf{k}, i\Omega_n) \rangle = \frac{T}{N} \chi(\mathbf{q}, i\nu_n) \delta_{\mathbf{q}, -\mathbf{k}} \delta_{\nu_n, -\Omega_n} \quad (2.12)$$

where $\langle \dots \rangle$ denotes an average over the probability distributions Eq. (2.4) and Eq. (2.6) for the vector and scalar cases respectively. In order to compare the scalar and vector molecular fields, we take the same form for their correlation function $\chi(\mathbf{q}, i\nu_n)$ and parametrize it as in Refs. [5,6]. In what follows, we set the lattice spacing a to unity. For real frequencies, we have

$$\chi(\mathbf{q}, \omega) = \frac{\chi_0 \kappa_0^2}{\kappa^2 + \tilde{q}^2 - i \frac{\omega}{\eta(\tilde{q})}} \quad (2.13)$$

where κ and κ_0 are the correlation wavevectors or inverse correlation lengths in units of the lattice spacing, with and without strong correlations, respectively. Let

$$\hat{q}_{\pm}^2 = 4 \pm 2(\cos(q_x) + \cos(q_y)) \quad (2.14)$$

We consider commensurate charge fluctuations and antiferromagnetic spin fluctuations, in which case the parameters \hat{q}^2 and $\eta(\hat{q})$ in Eq. (2.13) are defined as

$$\hat{q}^2 = \hat{q}_+^2 \quad (2.15)$$

$$\eta(\hat{q}) = T_0 \hat{q}_- \quad (2.16)$$

where T_0 is a characteristic temperature.

We also consider the case of ferromagnetic spin-fluctuations, where the parameters \hat{q}^2 and $\eta(\hat{q})$ in Eq. (2.13) are given by

$$\hat{q}^2 = \hat{q}_-^2 \quad (2.17)$$

$$\eta(\hat{q}) = T_0 \hat{q}_- \quad (2.18)$$

$\chi(\mathbf{q}, i\nu_n)$ is related to the imaginary part of the response function $Im\chi(\mathbf{q}, \omega)$, Eq. (2.13), via the spectral representation

$$\chi(\mathbf{q}, i\nu_n) = - \int_{-\infty}^{+\infty} \frac{d\omega}{\pi} \frac{Im\chi(\mathbf{q}, \omega)}{i\nu_n - \omega} \quad (2.19)$$

To get $\chi(\mathbf{q}, i\nu_n)$ to decay as $1/\nu_n^2$ as $\nu_n \rightarrow \infty$, as it should, we introduce a cutoff ω_0 and take $Im\chi(\mathbf{q}, \omega) = 0$ for $\omega \geq \omega_0$. A natural choice for the cutoff is $\omega_0 = \eta(\hat{q})\kappa_0^2$.

In our model, the single particle Green's function is the average over the probability distributions $\mathcal{P}[\mathbf{M}]$ (Eq. (2.4)) or $\mathcal{P}[\Phi]$ (Eq. (2.6)) of the fermion Green's function in a dynamical vector or scalar field.

$$\mathcal{G}(i\sigma\tau; j\sigma'\tau') = \int D\mathbf{M} \mathcal{P}[\mathbf{M}] G(i\sigma\tau; j\sigma'\tau'|[\mathbf{M}]) \quad (2.20)$$

$$\mathcal{G}(i\sigma\tau; j\sigma'\tau') = \int D\Phi \mathcal{P}[\Phi] G(i\sigma\tau; j\sigma'\tau'|[\Phi]) \quad (2.21)$$

where

$$G(i\sigma\tau; j\sigma'\tau'|[\mathbf{M}] \text{ or } [\Phi]) = -\langle T_{\tau} \{ \psi_{i\sigma}(\tau) \psi_{j\sigma'}^{\dagger}(\tau') \} \rangle \quad (2.22)$$

is the single particle Green's function in a dynamical molecular field and is discussed at length in Ref. [1]. In evaluating expressions Eqs. (2.20,2.21) one is summing over all Feynman diagrams corresponding to spin or charge-fluctuation exchanges [1,2,7]. The diagrammatic expansion of the Green's function in a dynamical field, Eq. (2.22) and its average, Eq. (2.20) are shown pictorially in Fig. 1. Since in our model no virtual fermion loops are present, there is no fermion sign problem [2].

In this paper we compare the results of the Monte Carlo simulations to various diagrammatic approximations for the same model. We denote by $\mathcal{G}_0(\mathbf{p}, i\omega_n)$ and $\mathcal{G}(\mathbf{p}, i\omega_n)$ the bare and dressed quasiparticle propagators respectively. They are given by

$$\mathcal{G}_0(\mathbf{p}, i\omega_n) = \frac{1}{i\omega_n - (\epsilon_{\mathbf{p}} - \mu)} \quad (2.23)$$

$$\mathcal{G}(\mathbf{p}, i\omega_n) = \frac{1}{i\omega_n - (\epsilon_{\mathbf{p}} - \mu) - \Sigma(\mathbf{p}, i\omega_n)} \quad (2.24)$$

where $\Sigma(\mathbf{p}, i\omega_n)$ is the quasiparticle self-energy and $\epsilon_{\mathbf{p}}$ the tight-binding dispersion relation obtained from Fourier transforming the hopping matrix t_{ij} in Eq. (2.1) and μ the chemical potential. We consider four approximations to the quasiparticle self-energy $\Sigma(\mathbf{p}, i\omega_n)$ whose diagrammatic representations are shown in Fig. 2.

In Fig. 2a, the self-energy is approximated by first order perturbation theory in the exchange of magnetic or charge fluctuations and denoted $\Sigma^{1pt}(\mathbf{p}, i\omega_n)$. Fig. 2b shows the Eliashberg approximation in which the self-energy denoted $\Sigma^{1sc}(\mathbf{p}, i\omega_n)$ is given by the first order self-consistent (or Brillouin-Wigner) perturbation theory. The expressions for $\Sigma^{1pt}(\mathbf{p}, i\omega_n)$ or $\Sigma^{1sc}(\mathbf{p}, i\omega_n)$ in the case of quasiparticles coupled to magnetic or charge fluctuations are identical (this is the reason for our choice of the factor $1/\sqrt{3}$ in Eq. (2.2)) and given by

$$\Sigma^{1pt}(\mathbf{p}, i\omega_n) = g^2 \frac{T}{N} \sum_{\mathbf{k}, \Omega_n} \chi(\mathbf{p} - \mathbf{k}, i\omega_n - i\Omega_n) \mathcal{G}_0(\mathbf{k}, i\Omega_n) \quad (2.25)$$

$$\Sigma^{1sc}(\mathbf{p}, i\omega_n) = g^2 \frac{T}{N} \sum_{\mathbf{k}, \Omega_n} \chi(\mathbf{p} - \mathbf{k}, i\omega_n - i\Omega_n) \mathcal{G}(\mathbf{k}, i\Omega_n) \quad (2.26)$$

where $\mathcal{G}_0(\mathbf{k}, i\Omega_n)$ and $\mathcal{G}(\mathbf{k}, i\Omega_n)$ are the bare and dressed quasiparticle Green's functions defined in Eq. (2.23) and Eq. (2.24) respectively. Fig. 2c shows the diagrammatic expansion

corresponding to second order perturbation theory and we denote the self-energy corresponding to that approximation $\Sigma^{2pt}(\mathbf{p}, i\omega_n)$. The second order self-consistent approximation to the quasiparticle self-energy, denoted $\Sigma^{2sc}(\mathbf{p}, i\omega_n)$, is shown diagrammatically in Fig. 2d. The expressions for $\Sigma^{2pt}(\mathbf{p}, i\omega_n)$ and $\Sigma^{2sc}(\mathbf{p}, i\omega_n)$ now depend on whether the quasiparticles are coupled to the vector Hubbard-Stratonovich field (magnetic fluctuations) or scalar Hubbard-Stratonovich field (charge fluctuations), because vertex corrections in the two cases do not have the same coefficient or even the same sign. The expressions for $\Sigma^{2pt}(\mathbf{p}, i\omega_n)$ and $\Sigma^{2sc}(\mathbf{p}, i\omega_n)$ for quasiparticles coupled to magnetic fluctuations are given by

$$\begin{aligned}
\Sigma^{2pt}(\mathbf{p}, i\omega_n) &= g^2 \frac{T}{N} \sum_{\mathbf{k}, \Omega_n} \chi(\mathbf{p} - \mathbf{k}, i\omega_n - i\Omega_n) \mathcal{G}_0(\mathbf{k}, i\Omega_n) \\
&+ g^2 \frac{T}{N} \sum_{\mathbf{k}, \Omega_n} \chi(\mathbf{p} - \mathbf{k}, i\omega_n - i\Omega_n) \mathcal{G}_0(\mathbf{k}, i\Omega_n) \Sigma^{1pt}(\mathbf{p}, i\omega_n) \mathcal{G}_0(\mathbf{k}, i\Omega_n) \\
&- \frac{1}{3} \left(g^2 \frac{T}{N} \right)^2 \sum_{\mathbf{k}, \Omega_n} \sum_{\mathbf{k}', \Omega'_n} \chi(\mathbf{p} - \mathbf{k}, i\omega_n - i\Omega_n) \mathcal{G}_0(\mathbf{k}, i\Omega_n) \mathcal{G}_0(\mathbf{k}', i\Omega'_n) \chi(\mathbf{k} - \mathbf{k}', i\Omega_n - i\Omega'_n) \\
&\times \mathcal{G}_0(\mathbf{p} - \mathbf{k} + \mathbf{k}', i\omega_n - i\Omega_n + i\Omega'_n) \tag{2.27}
\end{aligned}$$

$$\begin{aligned}
\Sigma^{2sc}(\mathbf{p}, i\omega_n) &= g^2 \frac{T}{N} \sum_{\mathbf{k}, \Omega_n} \chi(\mathbf{p} - \mathbf{k}, i\omega_n - i\Omega_n) \mathcal{G}(\mathbf{k}, i\Omega_n) \\
&- \frac{1}{3} \left(g^2 \frac{T}{N} \right)^2 \sum_{\mathbf{k}, \Omega_n} \sum_{\mathbf{k}', \Omega'_n} \chi(\mathbf{p} - \mathbf{k}, i\omega_n - i\Omega_n) \mathcal{G}(\mathbf{k}, i\Omega_n) \mathcal{G}(\mathbf{k}', i\Omega'_n) \chi(\mathbf{k} - \mathbf{k}', i\Omega_n - i\Omega'_n) \\
&\times \mathcal{G}(\mathbf{p} - \mathbf{k} + \mathbf{k}', i\omega_n - i\Omega_n + i\Omega'_n) \tag{2.28}
\end{aligned}$$

In the case of the scalar Hubbard-Stratonovich field, or coupling to charge fluctuations, the corresponding expressions are

$$\begin{aligned}
\Sigma^{2pt}(\mathbf{p}, i\omega_n) &= g^2 \frac{T}{N} \sum_{\mathbf{k}, \Omega_n} \chi(\mathbf{p} - \mathbf{k}, i\omega_n - i\Omega_n) \mathcal{G}_0(\mathbf{k}, i\Omega_n) \\
&+ g^2 \frac{T}{N} \sum_{\mathbf{k}, \Omega_n} \chi(\mathbf{p} - \mathbf{k}, i\omega_n - i\Omega_n) \mathcal{G}_0(\mathbf{k}, i\Omega_n) \Sigma^{1pt}(\mathbf{p}, i\omega_n) \mathcal{G}_0(\mathbf{k}, i\Omega_n) \\
&+ \left(g^2 \frac{T}{N} \right)^2 \sum_{\mathbf{k}, \Omega_n} \sum_{\mathbf{k}', \Omega'_n} \chi(\mathbf{p} - \mathbf{k}, i\omega_n - i\Omega_n) \mathcal{G}_0(\mathbf{k}, i\Omega_n) \mathcal{G}_0(\mathbf{k}', i\Omega'_n) \chi(\mathbf{k} - \mathbf{k}', i\Omega_n - i\Omega'_n) \\
&\times \mathcal{G}_0(\mathbf{p} - \mathbf{k} + \mathbf{k}', i\omega_n - i\Omega_n + i\Omega'_n) \tag{2.29}
\end{aligned}$$

$$\Sigma^{2sc}(\mathbf{p}, i\omega_n) = g^2 \frac{T}{N} \sum_{\mathbf{k}, \Omega_n} \chi(\mathbf{p} - \mathbf{k}, i\omega_n - i\Omega_n) \mathcal{G}(\mathbf{k}, i\Omega_n)$$

$$\begin{aligned}
& + \left(g^2 \frac{T}{N} \right)^2 \sum_{\mathbf{k}, \Omega_n} \sum_{\mathbf{k}', \Omega'_n} \chi(\mathbf{p} - \mathbf{k}, i\omega_n - i\Omega_n) \mathcal{G}(\mathbf{k}, i\Omega_n) \mathcal{G}(\mathbf{k}', i\Omega'_n) \chi(\mathbf{k} - \mathbf{k}', i\Omega_n - i\Omega'_n) \\
& \times \mathcal{G}(\mathbf{p} - \mathbf{k} + \mathbf{k}', i\omega_n - i\Omega_n + i\Omega'_n)
\end{aligned} \tag{2.30}$$

In Eqs. (2.27,2.28,2.29,2.30), $\mathcal{G}_0(\mathbf{k}, i\Omega_n)$ and $\mathcal{G}(\mathbf{k}, i\Omega_n)$ are the bare and dressed quasiparticle Green's functions defined in Eq. (2.23) and Eq. (2.24) respectively.

III. RESULTS

The quasiparticle dispersion relation for the two-dimensional square lattice is obtained from Eq. (2.1). We measure all energies and temperatures in units of the nearest-neighbor hopping parameter t . We set the next-nearest-neighbor hopping parameter $t' = -0.45t$. The chemical potential is adjusted so that the electronic band filling is $n = 0.9$. The dimensionless parameters describing the molecular field correlations are $g^2\chi_0/t$, T_0/t , κ_0 and κ . We chose a representative value for $\kappa_0^2 = 12$, and set $T_0 = 0.67t$ as in the earlier work [1]. For an electronic bandwidth of $1eV$, $T_0 \approx 1000^\circ\text{K}$. We only consider one value of the coupling constant $g^2\chi_0/t = 2$. In the random phase approximation, the magnetic instability would be obtained for a value of $g^2\chi_0/t$ of the order of 10. We consider what happens to the quasiparticle spectrum at a fixed temperature $T = 0.25t$ as the inverse correlation length κ changes, as in Ref. [1].

All the calculations were done on a 8 by 8 spatial lattice. In the Monte Carlo calculations we used 41 imaginary time slices, or equivalently 41 Matsubara frequencies for the molecular fields, $\mathbf{M}(\mathbf{q}, i\nu_n)$ and $\Phi(\mathbf{q}, i\nu_n)$ ($\nu_n = 2\pi nT$, with $n = 0, \pm 1, \dots, \pm 20$). In the diagrammatic calculations, we used between 40 to 60 fermion Matsubara frequencies.

By analytic continuation of the single particle Green's function $\mathcal{G}(\mathbf{k}, \tau)$ or $\mathcal{G}(\mathbf{k}, i\omega_n)$ one can obtain the quasiparticle spectral function $A(\mathbf{k}, \omega) = -\frac{1}{\pi} \text{Im} \mathcal{G}_R(\mathbf{k}, \omega)$ and the tunneling density of states $N(\omega) = \frac{1}{N} \sum_{\mathbf{k}} A(\mathbf{k}, \omega)$, where $\mathcal{G}_R(\mathbf{k}, \omega)$ is the retarded single particle Green's function. In the case of diagrammatic approximations, $\mathcal{G}(\mathbf{k}, i\omega_n)$ is analytically continued from imaginary to real frequencies by means of Padé approximants [8]. The imaginary time

Monte Carlo data is analytically continued with the Maximum Entropy method [9], using the same methodology as in the earlier work [1].

A. Antiferromagnetic spin-fluctuations

Figs. 3,4 and 5 show the comparison, for different values of κ^2 , between the nonperturbative calculations of the quasiparticle spectral function $A(\mathbf{k}, \omega)$ and tunneling density of states $N(\omega)$ and those obtained from the approximations $\Sigma^{1pt}(\mathbf{p}, i\omega_n)$, $\Sigma^{2pt}(\mathbf{p}, i\omega_n)$, $\Sigma^{1sc}(\mathbf{p}, i\omega_n)$, and $\Sigma^{2sc}(\mathbf{p}, i\omega_n)$ to the quasiparticle self-energy.

For $\kappa^2 = 4$, namely relatively weak antiferromagnetic correlations, the spectral functions at $\mathbf{k} = (\pi, 0)$ and $\mathbf{k} = (\pi/4, \pi/4)$ and tunneling density of states obtained from the various diagrammatic approximations agree qualitatively with the Monte Carlo results. There are, however, noticeable quantitative differences, much more so in the spectral function $A(\mathbf{k}, \omega)$ than in the tunneling density of states $N(\omega)$. The quantitative differences between the diagrammatic and nonperturbative calculations of $A(\mathbf{k}, \omega)$ are smaller for $\mathbf{k} = (\pi/4, \pi/4)$ than for $\mathbf{k} = (\pi, 0)$. This is not unexpected since the quasiparticle momentum $\mathbf{k} = (\pi/4, \pi/4)$ is further away from the hot spots (momenta \mathbf{p} such that both \mathbf{p} and $\mathbf{p} \pm (\pi, \pi)$ are on the Fermi surface) than $\mathbf{k} = (\pi, 0)$. The nonperturbative $A(\mathbf{k}, \omega)$ is broader in frequency than all of the diagrammatic approximations. This implies that the effect of all antiferromagnetic spin-fluctuation exchanges leads to a stronger effective interaction than the first and second order processes alone. It is instructive to compare the various perturbation-theoretic approximations amongst themselves. One notices the relatively small differences between the self-consistent and simple perturbation theory, in first and second order. This is not surprising for weak magnetic correlations. The dressing of the quasiparticle propagators in self-consistent calculations is expected to lead to weaker effective interactions, and thus a more sharply peaked $A(\mathbf{k}, \omega)$ as is indeed observed in Figs. 3a,b. Note, however, that for the different approximations, the Fermi surface can be renormalized differently by the interactions, i.e. have a slightly different shape. Therefore, how close a given quasiparti-

cle momentum \mathbf{k} is to the Fermi surface can depend on the approximation and this alone could make the spectral function sharper or broader. Figs. 3a,b show that there is more of a difference between the second order results, which contain vertex corrections, and the first order calculations than between self-consistent and perturbation-theoretic results at the same order. Moreover, the inclusion of vertex corrections leads to broader in ω spectral functions which are in better agreement with the Monte Carlo calculations, the second order perturbation theory result being the better of the two. First order vertex corrections are seen to lead to an enhancement of the spin-fluctuation interaction, as in Refs. [10,11], and the comparison between the second order and Monte Carlo results, for which the spectral function is broader in ω than any of the diagrammatic approximations, shows that the multiple spin-fluctuation exchanges not included in the diagrammatic approximations lead to an even stronger enhancement of the effective quasiparticle interaction.

As $\kappa^2 \approx 1$, the quasiparticle mean free path becomes of the order of the magnetic correlation length for some wavevectors near the Fermi surface, the quasiparticles then can't tell there is no long-range order, and this marks the onset of pseudogap behavior [1]. As Fig. 4 shows for $\kappa^2 = 1$, this developing pseudogap in the spectral function $A(\mathbf{k}, \omega)$ at $\mathbf{k} = (\pi, 0)$ (Fig. 4a) and in the tunneling density of states $N(\omega)$ (Fig. 4c) found in the nonperturbative Monte Carlo calculations is not seen in any of the diagrammatic approximations considered here, which therefore fail qualitatively. Also note that for $\kappa^2 = 1$, there is nearly as much difference between the perturbation theoretic and self-consistent approximations of the same order as there are between calculations of the same type at first and second order. For $\mathbf{k} = (\pi/4, \pi/4)$, away from the hot spots where the quasiparticle mean free path is longer and the pseudogap not present, we note again that the second order perturbation theory for $A(\mathbf{k}, \omega)$ (Fig. 4b) is closer to the Monte Carlo result than the other approximations considered here. As for the case $\kappa^2 = 4$, Figs. 4a,b show that the first order vertex corrections included in the second order calculations lead to an enhancement of the bare spin-fluctuation interaction which is signalled by a broader in ω quasiparticle spectral function. Furthermore, Fig. 4b shows that since the Monte Carlo $A(\mathbf{k}, \omega)$ is broader than even the second order

results, the higher order spin-fluctuation exchanges which are neglected in the diagrammatic approximations lead to a further enhancement of the effective quasiparticle interaction, as was noted for $\kappa^2 = 4$.

At $\kappa^2 = 0.25$, shown in Fig. 5, one is well into the pseudogap regime. A look at Fig. 5a might suggest that since the second order perturbation theory answer for $A(\mathbf{k}, \omega)$ has a double peak structure, this approximation contains enough of the physics to produce the pseudogap state, albeit at a smaller value of κ^2 than in the nonperturbative calculation. However, Fig. 5c shows this is not the case. The second order perturbation-theoretic approximation fails to show the suppression of the quasiparticle tunneling density of states at the Fermi level ($\omega = 0$) found in the nonperturbative calculation. The conclusion one can draw is that none of the diagrammatic approximations to the self-energy considered here can properly describe the pseudogap state. Moreover, Figs. 5a,b show signs that the simple perturbation theory for this choice of model parameters is not well behaved at all, given the large differences between the first and second order results. The self-consistent, or renormalized, perturbation theory on the other hand shows much smaller changes between first and second order. But even if it converges, Figs. 5a,c indicate that for $\kappa^2 = 0.25$ it most likely converges to the wrong answer.

B. Ferromagnetic spin-fluctuations

Figs. 6,7, and 8 show our results for the quasiparticle spectral function $A(\mathbf{k}, \omega)$ and tunneling density of states $N(\omega)$ for several values of κ^2 . For $\kappa^2 = 4$, or relatively weak ferromagnetic correlations, Fig. 6 shows that the diagrammatic approximations all qualitatively agree with the Monte Carlo results. As in the corresponding antiferromagnetic case, there are larger quantitative differences between the perturbation-theoretic and nonperturbative calculations for the spectral function $A(\mathbf{k}, \omega)$ (Figs. 6a,b) than for the tunneling density of states $N(\omega)$ (Fig. 6c). One notes a number of other similarities between the results of Fig. 6 and the corresponding antiferromagnetic case, shown in Fig. 4: (i) the

second order perturbation theory results for $A(\mathbf{k}, \omega)$ give the best agreement with the non-perturbative calculation, (ii) since the spectral function in either second order calculation, which include vertex corrections, is broader in ω than the corresponding first order result, we conclude that first order vertex corrections lead to an enhancement of the effective quasiparticle interaction, (iii) the spectral function obtained by Monte Carlo sampling of the Gaussian dynamical molecular fields is even broader than the second order results, which is an indication that higher order spin-fluctuation exchanges not included in the diagrammatic approximations considered lead to a further enhancement of the effective quasiparticle interaction.

A comparison between Figs. 4 and 6 shows that the diagrammatic calculations, in particular the second order ones, provide a better approximation to the Monte Carlo results in the ferromagnetic case than for antiferromagnetic spin fluctuations. This is not unexpected since the dynamical exponent z is larger for ferromagnetic than antiferromagnetic spin fluctuations. Hence the effective dimension $d + z = 5$ in the ferromagnetic versus $d + z = 4$ in the antiferromagnetic case and the standard theory of quantum critical phenomena [12] leads one to expect weaker corrections for higher effective dimensions. The perturbative calculations qualitatively fail at $\kappa^2 \approx 1$ in the antiferromagnetic case and on the basis of the above arguments one would expect that the breakdown of perturbation theory in the case of ferromagnetic fluctuations, if it happens, would occur for a smaller value of κ^2 . Indeed, at $\kappa^2 = 1$, Fig. 7 shows that the diagrammatic calculations still agree qualitatively with the Monte Carlo results although there are larger quantitative differences than in the case $\kappa^2 = 4$ shown in Fig. 6. Fig. 7b gives a hint that the perturbation theory in this case is not well behaved, because the results of the first and second order calculations differ greatly. The self-consistent, or renormalized, perturbation theory seems better behaved, as in the antiferromagnetic case, because the difference between the first and second order calculations are much less pronounced.

Our results for $\kappa^2 = 0.25$ are shown in Fig. 8. The spectral function $A(\mathbf{k}, \omega)$ obtained from the nonperturbative Monte Carlo calculations shows a double peak structure. This

has been interpreted in Ref. [1] as an effective spin-splitting of the quasiparticle spectrum induced by the local ferromagnetic order. The self-consistent calculations do not show a double peak structure in either first or second order and thus qualitatively fail. The first order perturbation-theoretic result for $A(\mathbf{k}, \omega)$ show some hint of a double peak structure but a look at Fig. 8c reveals that this approximation fails to produce the dip in the tunneling density of states at the Fermi level $\omega = 0$ and therefore does not have the correct physics built in. And similarly, the second order perturbation-theoretic result barely shows a double peak structure at $\mathbf{k} = (\pi, 0)$ (Fig. 8a) and also fails to reproduce the local minimum in the tunneling density of state at the Fermi level $\omega = 0$ (Fig. 8c).

C. Charge fluctuations

Our results for the quasiparticle spectral function $A(\mathbf{k}, \omega)$ and tunneling density of states $N(\omega)$ are shown in Figs. 9,10 and 11. The reader will notice that the results of the second order perturbation theory (self-consistent or not) are not displayed in the figures. The reason is that both second order approximations, $\Sigma^{2pt}(\mathbf{p}, i\omega_n)$ and $\Sigma^{2sc}(\mathbf{p}, i\omega_n)$, for the model parameters considered here, effectively violate causality requirements in that the Eliashberg renormalization factor $Z(\mathbf{p}, i\omega_n)$ becomes less than one. In terms of the quasiparticle self-energy $\Sigma(\mathbf{p}, i\omega_n)$, $Z(\mathbf{p}, i\omega_n) = 1 - \frac{1}{\omega_n} \text{Im}\Sigma(\mathbf{p}, i\omega_n) = 1 - \int_{-\infty}^{+\infty} \frac{d\omega}{\pi} \frac{\text{Im}\Sigma_R(\mathbf{p}, \omega)}{\omega^2 + \omega_n^2}$ where $\text{Im}\Sigma_R(\mathbf{p}, \omega)$ is the imaginary part of the retarded self-energy and we have made use of the spectral representation for the self-energy $\Sigma(\mathbf{p}, i\omega_n) = - \int_{-\infty}^{+\infty} \frac{d\omega}{\pi} \frac{\text{Im}\Sigma_R(\mathbf{p}, \omega)}{i\omega_n - \omega}$. Causality demands that the retarded Green's function be analytic in the upper-half complex frequency plane and therefore that the imaginary part of the retarded self-energy be always less than or equal to zero ($\text{Im}\Sigma_R(\mathbf{p}, \omega) \leq 0$) for all values of \mathbf{p}, ω . This in turn means that $Z(\mathbf{p}, i\omega_n) \geq 1$ for all values of \mathbf{p}, ω . One can write the second order Eliashberg renormalization factor $Z^{(2)}(\mathbf{p}, i\omega_n) = 1 + \Delta Z^{(1)}(\mathbf{p}, i\omega_n) + \Delta Z^{(2)}(\mathbf{p}, i\omega_n)$, where $\Delta Z^{(i)}(\mathbf{p}, i\omega_n)$ is the change in $Z(\mathbf{p}, i\omega_n)$ coming from the i^{th} order diagrams. $\Delta Z^{(1)}(\mathbf{p}, i\omega_n)$ is always greater than zero and therefore poses no problem as far as the condition $Z(\mathbf{p}, i\omega_n) \geq 1$ is concerned. In the

charge-fluctuation case, as was explained in Ref. [1], the first order vertex correction has the opposite sign compared to the spin-fluctuation case, and leads to a suppression of the effective quasiparticle interaction. The enhancement of the quasiparticle spin-fluctuation vertex comes from the transverse magnetic fluctuations that manage to overcome the reduction of the effective coupling due to the longitudinal fluctuations. Because of this cancellation effect, not only is the sign of the first order vertex correction different in the magnetic case, it is also smaller in magnitude than in the charge-fluctuation case, under otherwise similar conditions, as can be seen from the factor $1/3$ in Eqs. (2.27,2.28) not present in the corresponding charge-fluctuation case in Eqs. (2.29,2.30). The different sign of the vertex corrections in the charge and magnetic cases means that while in the magnetic case $\Delta Z^{(2)}(\mathbf{p}, i\omega_n) \geq 0$ and at second order $Z^{(2)}(\mathbf{p}, i\omega_n)$ is always ≥ 1 , in the charge fluctuation case $\Delta Z^{(2)}(\mathbf{p}, i\omega_n) \leq 0$. For the range of model parameters considered here, we find that the second order contribution to the Eliashberg renormalization factor is greater in magnitude than the first order contribution, $|\Delta Z^{(2)}(\mathbf{p}, i\omega_n)| > |\Delta Z^{(1)}(\mathbf{p}, i\omega_n)|$ and since it has the opposite sign, $Z^{(2)}(\mathbf{p}, i\omega_n) = 1 + \Delta Z^{(1)}(\mathbf{p}, i\omega_n) + \Delta Z^{(2)}(\mathbf{p}, i\omega_n) \leq 1$. Note that the nonperturbative calculations always satisfy $Z(\mathbf{p}, i\omega_n) \geq 1$, and the problem only arises in the perturbative approximation and is a sign that, for the range of model parameters considered here, the perturbation expansion for the charge-fluctuation case is quite badly behaved, possibly even more so than for magnetic fluctuations

Figs. 9, 10 and 11 show that the spectral function $A(\mathbf{k}, \omega)$ obtained from the non-perturbative calculations is sharper than those produced by the first order self-consistent calculations. This means that for $g^2\chi_0/t = 2$ and $T_0 = 0.67t$ the first and higher order vertex corrections suppress the effective quasiparticle interaction for κ^2 in the range $[0.25, 4.00]$. It is therefore not surprising that there are no qualitative differences between the nonperturbative and diagrammatic calculations for these values of the model parameters. As noted in Ref. [1], one would also, on general grounds, expect pseudogap effects in the charge-fluctuation case, but these would occur for smaller values of κ^2 than for quasiparticles coupled to antiferromagnetic spin-fluctuations.

A comparison between Figs. 9a and 9b show that while there are large quantitative differences between the first order and the Monte Carlo results for $A(\mathbf{k}, \omega)$ at $\mathbf{k} = (\pi, 0)$ and even for this relatively large value of κ^2 , the first order results agree quite well with the nonperturbative calculations away from the hot spots at $\mathbf{k} = (\pi/4, \pi/4)$. For relatively weak charge correlations, $\kappa^2 = 4$, there is little difference between the perturbation-theoretic and self-consistent results. As κ^2 decreases, these differences become pronounced, as Fig. 11 shows. This could indicate the breakdown of the perturbation expansion.

IV. DISCUSSION

In Ref. [1], we showed that the magnetic pseudogap induced by a coupling to antiferromagnetic spin-fluctuations and the spin-splitting of the quasiparticle peak induced by a coupling to ferromagnetic spin fluctuations were not captured by the first order self-consistent, or Eliashberg, approximation. The main result of this paper, is that these phenomena also lie beyond the two magnetic-fluctuation exchange theories (self-consistent or not), which contain first order vertex corrections. While this does obviously not constitute a proof, these results are consistent with the conjecture expressed in Ref. [1] that the pseudogap effects found in the Monte Carlo calculations are intrinsically nonperturbative in nature. Since the calculations reported here show that the first order vertex corrections alone do not produce a magnetic pseudogap, the physics of that state must then mainly come from the higher order spin-fluctuation exchange processes. The results presented here and in Ref. [1] also indicate that a CDW pseudogap induced by coupling to the scalar dynamical molecular field (Eq. (2.3)) must also originate from high order charge-fluctuation exchange processes. Close enough to a second order CDW transition, the diverging CDW correlation length is bound to exceed the characteristic length scale for quasiparticles and the calculations of Ref. [13] showed that when this happens a pseudogap opens in the quasiparticle spectrum. The first order vertex correction can't produce the pseudogap state, since as we have seen, in the case of charge fluctuations it leads to a suppression of the interaction. In fact we even found

that for the range of model parameters considered here, the second order diagrams more than cancel the contribution from the first order terms leading to a second order Eliashberg renormalization parameter $Z(\mathbf{p}, i\omega_n) \leq 1$, which is inconsistent with causality requirements. Moreover, we expect this "over-cancellation" effect to get worse as κ^2 gets smaller than the lowest value considered here, $\kappa^2 = 0.25$. Since $Z(\mathbf{p}, i\omega_n)$ must be ≥ 1 when all the diagrams are summed up, as in the Monte Carlo simulations, one can conclude that the higher than second order terms must give a contribution ΔZ to Z which is positive. Therefore, higher order charge-fluctuation exchange processes produce an enhancement of the effective quasiparticle interaction, as in the magnetic case, and it must be through this enhancement of the effective interaction that a pseudogap can appear in the quasiparticle spectrum on the border of long-range CDW order.

These observations lead one to a unified picture of the pseudogap state for quasiparticles coupled to spin or charge fluctuations. When the dynamical molecular field correlation length exceeds the characteristic length scale for quasiparticles, either the thermal de Broglie wavelength [13–15] or mean free path [1], the quasiparticles effectively see long range order and this marks the onset of the pseudogap state. This state must be produced by high order spin or charge-fluctuation exchanges which contain subtle quantum mechanical coherence effects. In the magnetic fluctuation case, the first order vertex correction favors the pseudogap state, while in the charge fluctuation case it suppresses it. This implies one has to be closer to the boundary of long-range charge order to observe a pseudogap than one has to be to the boundary of magnetic long-range order, under otherwise similar conditions. There still remains, however, the problem of understanding what property of the full vertex function $\Gamma_{\alpha,\gamma}^i(\mathbf{x}, \tau; \mathbf{x}', \tau' | \mathbf{x}'' , \tau'') = \langle T_\tau \psi_\alpha(\mathbf{x}, \tau) \psi_\gamma^\dagger(\mathbf{x}', \tau') M^i(\mathbf{x}'', \tau'') \rangle$ is missing in its first order approximation. This question is currently under investigation.

Our physical picture of the pseudogap state emerging from quantum mechanical coherence effects contained in high order Feynman diagrams is to be contrasted with the results of Refs. [16–18] where a suppression of the quasiparticle tunneling density of states at the Fermi level is obtained in the single spin or charge-fluctuation exchange approximation. This

effect is typically obtained with relatively large magnetic or charge correlation lengths. In our model, the calculations reported here and in Ref. [1] show that as one approaches the border of magnetic long-range order, $\kappa^2 \rightarrow 0$, the multiple spin-fluctuation exchange processes become important long before a suppression of the quasiparticle tunneling density of states at the Fermi level is seen in the first order perturbation-theoretic and self-consistent calculations. The above finding is likely to be valid more generally, since the intuitive arguments for the physical origin of the pseudogap [1,13–15] lead one to expect the breakdown of Migdal’s theorem to be a generic occurrence near a spin or charge instability. There is also an important difference between a vertex correction induced pseudogap and a single-fluctuation exchange pseudogap. In the latter case, there is no essential distinction between spin and charge fluctuations, in that at the single-fluctuation exchange level, for a given fluctuation spectrum the spin and charge-fluctuation theories of the quasiparticle spectral function can be made identical by an appropriate scaling of the coupling constant to the molecular field. This is no longer the case when vertex corrections are included, since these actually depend on the nature of the Hubbard-Stratonovich field, in our case vector versus scalar. The distinction could turn out to be essential, since we find, for a range of model parameters, that a pseudogap is observed for quasiparticles coupled to spin fluctuations but not in the corresponding charge-fluctuation case.

Moukouri et al. [15] have developed a many-body theory of the precursor pseudogap to the Mott transition in the half-filled Hubbard model. Their theory is inspired by the fluctuation exchange approximation (FLEX) [19] in which bare spin and charge susceptibilities are used to build up the effective quasiparticle interaction, corresponding to $g^2\chi(\mathbf{q}, \omega)$ in our model. The key respect in which the theory of Moukouri et al. [15] differs from FLEX is that the coupling to spin and charge fluctuations are not given by the bare on-site Coulomb repulsion, but by renormalized parameters determined self-consistently in such a way that an exact relationship between the single and two-particle Green’s functions is satisfied. This last step goes beyond perturbation theory and it is therefore plausible that the precursor pseudogap to the Mott transition seen in the Monte Carlo simulations of the half-filled

Hubbard model [15] is also nonperturbative in origin. The analog of their scheme for the present model would be the use of the first order perturbation theory approximation for the quasiparticle self-energy $\Sigma^{(1pt)}(\mathbf{p}, \omega)$, Eq. (2.25) and a simultaneous renormalization of the coupling constant g and the correlation wavevector κ^2 . A renormalization of the coupling constant g could account for all vertex corrections provided they are local in space and time.

One can indeed get a pseudogap in the tunneling density of states with the first order perturbation theory approximation to $\Sigma(\mathbf{p}, \omega)$ (Eq. (2.25)), as in Refs. [16,17], provided κ^2 is renormalized to lower values and g renormalized to higher ones. The onset of pseudogap behavior in the Monte Carlo simulations occurs at $\kappa^2 \approx 1$ for $g^2\chi_0/t = 2$. The first order perturbation-theoretic calculation requires a renormalization by a factor of three to four of both parameters ($g^2\chi_0/t \rightarrow 6$ and $\kappa^2 \rightarrow 0.25$) to get a suppression of the tunneling density of states $N(\omega)$ at $\omega = 0$, but the fit to the Monte Carlo results is not very good, in that the perturbation-theoretic result for $N(\omega)$ extends over a much wider range of frequencies ω . Moreover, the perturbation-theoretic spectral function at $\mathbf{k} = (\pi, 0)$ does not show the double peak structure seen in the Monte Carlo simulations. We have not been able to get good fits to the tunneling density of states using this renormalization scheme. And typically the fits to the spectral function $A(\mathbf{k}, \omega)$ were worse than those to the tunneling density of states $N(\omega)$. One would also naively expect a sensible renormalization scheme that goes beyond the one-loop level to lead to renormalized values of κ^2 larger than the bare value. The renormalized theory should be further away from the magnetic instability than the one-loop approximation rather than closer to it, since ideally one would like the improved theory to satisfy the Mermin-Wagner theorem in two dimensions. If κ^2 were to be increased by the renormalization scheme, in order to obtain a pseudogap in $N(\omega)$ one would likely need a large renormalization of the coupling g and such a scheme for the present model, which is different than the one considered in Ref. [15], does not look promising to the author. Also note that in the work reported here, the effective interaction is not determined self-consistently as in the calculations of Moukouri et al. [15]. The extent to which a self-consistent calculation of the magnetic or charge response function $\chi(\mathbf{q}, \omega)$ affects the results described here is not

known, but we hope to address this issue in the near future.

In Ref. [1], we pointed out that in the case of quasiparticles coupled to ferromagnetic spin fluctuations, our results are at variance with expectations based on the standard theory of quantum critical phenomena [12]. Since the dynamical exponent $z = 3$, in $d = 2$ spatial dimensions, the effective dimension is $d + z = 5$ and is greater than the upper critical dimension $d_c = 4$ above which one would expect the first order theory to be at least qualitatively correct. But our nonperturbative results show that at least for small enough κ^2 , the first order theory qualitatively breaks down. For antiferromagnetic and charge fluctuations, $d + z = 4$, the marginal case, and hence the qualitative breakdown of the first order approximation isn't necessarily inconsistent with the standard theory. However, the scaling relations derived in Ref. [12] rely on the applicability of perturbation theory. If the pseudogap effects are indeed intrinsically nonperturbative in nature, a conjecture that is consistent with the present work, it opens the possibility that the physics in the proximity of a quantum critical point is dominated by nonperturbative quantum mechanical effects and therefore even richer than anticipated in the earlier work [12]. A number of new ideas in this field have recently been proposed [20,21] and a discussion of some fundamental problems associated with quantum critical points can be found in Ref. [22].

V. OUTLOOK

We studied a nonperturbative formulation of the magnetic interaction model, in which quasiparticles are coupled to a Gaussian distributed dynamical molecular exchange field. Far from the magnetic boundary, the multiple magnetic fluctuation exchange processes do not bring about qualitative changes to the quasiparticle spectrum. But as one gets closer to the border of long-range magnetic order, we find, for a range of model parameters, that Migdal's theorem doesn't apply and the quasiparticle spectrum is qualitatively different from its Eliashberg approximation. Moreover, we find that going one step beyond the single spin-fluctuation exchange approximation and including first order vertex corrections,

self-consistently or not, doesn't help to reproduce the qualitative changes seen in the non-perturbative calculations. Near the magnetic boundary, the simple perturbation expansion shows signs it is not well behaved, since the second order results differ greatly from their first order counterparts. The self-consistent, or renormalized perturbation expansion, which effectively consists in a reordering of the diagrammatic perturbation theory, is better behaved in that the differences between first and second order are much less pronounced. However, even if the renormalized perturbation expansion converges, our results show that it is quite likely to converge to the wrong answer, which could be explained if the original perturbation expansion is divergent.

The intuitive argument for the onset of pseudogap behavior [1,13–15], namely that if the distance quasiparticles can travel during their lifetime becomes shorter than the molecular field correlation length, these quasiparticles effectively see long-range order, does not explain the failure of the single spin-fluctuation exchange approximation. As we pointed out in Ref. [1], one can get in the regime where the mean-free path gets shorter than $1/\kappa$ in the Eliashberg approximation, but fail to observe a pseudogap in this regime. Since we have not been able to produce a good fit to the Monte Carlo simulations by including either first order or vertex corrections that are local in space and time, i.e by a renormalization of the coupling constant g to the molecular field, we conjecture that the physical origin of the pseudogap state found in the present calculations lies in non-local vertex corrections produced by high order spin-fluctuation exchanges. These vertex corrections effectively induce a quasiparticle coupling to the dynamical molecular field that is non-local in both space and time. The above conjecture raise the question of what essential property of the vertex function is not captured by its first order approximation. A study of the vertex function along the same lines as the work reported here for the single particle Green's function should provide further insights into this problem. We are currently investigating this difficult but important question.

VI. ACKNOWLEDGMENTS

I would like to thank P. Coleman, J.R. Cooper, P.B. Littlewood, G.G. Lonzarich, J. Loram, and D. Pines for discussions on this and related topics. We acknowledge the support of the EPSRC, the Newton Trust and the Royal Society.

REFERENCES

- [1] P. Monthoux, Phys. Rev. B **68**, 064408 (2003).
- [2] P. Monthoux, Phil. Mag. B **79**, 15 (1999).
- [3] T.Moriya, Y. Takahashi and K. Ueda, J. Phys. Soc. Jpn. **52**, 2905 (1990). P. Monthoux, A.V. Balatsky and D. Pines, Phys. Rev. Lett. **67**, 3448 (1991).
- [4] E.R. Dobbs, "Helium Three", Oxford University Press (2001).
- [5] P. Monthoux and G.G. Lonzarich, Phys. Rev. B **59**, 14598 (1999).
- [6] P. Monthoux and G.G. Lonzarich, Phys. Rev. B **63**, 054529 (2001).
- [7] A. Posazhennikova and P. Coleman, Phys. Rev. B **67**, 165109 (2003).
- [8] H.J. Vidberg and J.W. Serene, J. Low Temp. Phys. **29**, 179 (1977).
- [9] M. Jarrell and J.E. Gubernatis, Phys. Rep. **269**, 134 (1996).
- [10] P. Monthoux, Phys. Rev. B **55**, 15261 (1997).
- [11] A.V. Chubukov, P. Monthoux and D.R. Morr, Phys. Rev. B **56**, 7789 (1997).
- [12] J.A. Hertz, Phys. Rev. B **14**, 1165 (1976). A.J. Millis, Phys. Rev. B **48**, 7183 (1993).
- [13] P. Monthoux and D.J. Scalapino, Phys. Rev. B **65**, 235104 (2002).
- [14] Y.M. Vilk and A.-M. S. Tremblay, J. Phys. I, France **7**, 1309 (1997).
- [15] S. Moukouri, S. Allen, F. Lemay, B. Kyung, D. Poulin. Y. M. Vilk and A.-M. S. Tremblay, Phys. Rev. B **61**, 7887 (2000).
- [16] A.P. Kampf and J.R. Schrieffer, Phys. Rev. B **41**, 6399 (1990).
- [17] P. Prelovsek and R. Ramsak, Phys. Rev. B **65**, 174529 (2002).
- [18] P.A. Lee, T.M. Rice and P.W. Anderson, Phys. Rev. Lett. **31**, 462 (1973).

- [19] N.E. Bickers and D.J. Scalapino, *Ann. Phys. (N.Y.)* **193**, 206 (1989).
- [20] P. Coleman and C. Pepin, *Physica B* **312**, 383 (2002).
- [21] Q.M. Si, S. Rabello, K. Ingersent, J.L. Smith, *Nature* **413**, 804 (2001).
- [22] R.B. Laughlin, G.G. Lonzarich, P. Monthoux and D. Pines, *Adv. Phys.* **50**, 361 (2001).

FIGURES

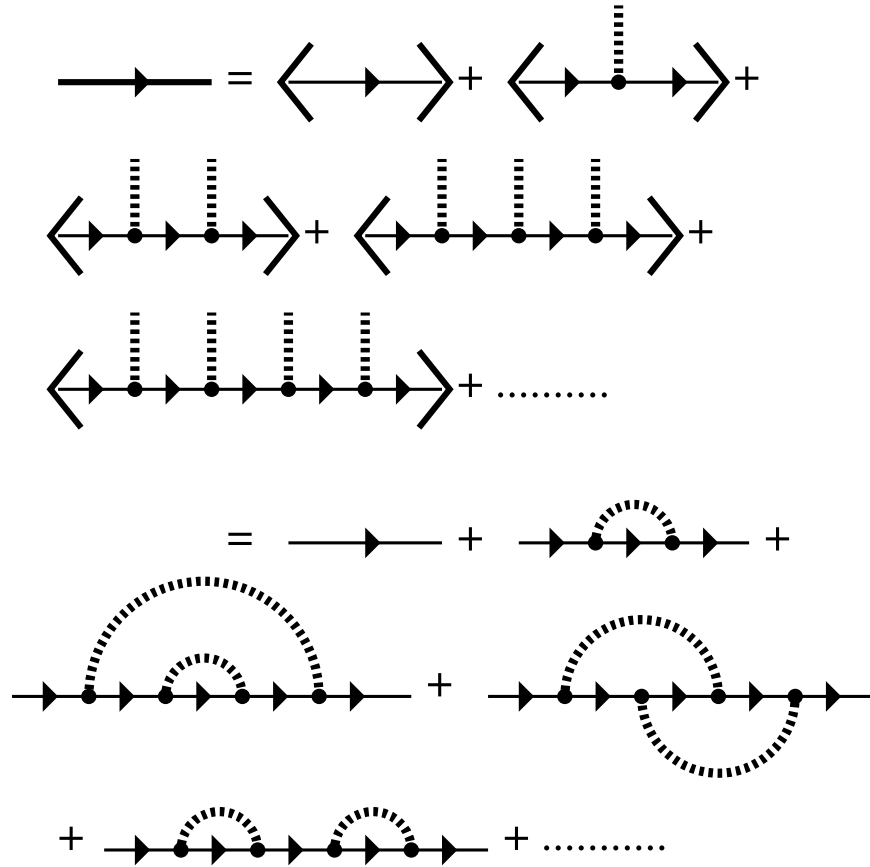


FIG. 1. Diagrammatic expansion for the single particle Green's function. The dashed line connected at one end only to the solid line represents the interaction of the fermions with the dynamical molecular field and the brackets the average over the Gaussian distribution of these fields. The averaging over the distribution of molecular fields is carried out by pairing the dashed lines in all possible ways, each pairing giving a factor proportional to the two-point correlation function of the molecular field, the dynamical susceptibility $\chi(\mathbf{q}, i\nu_n)$ according to Eqs. (2.11,2.12). The lower part of the figure shows the pairings one obtains up to two spin or charge-fluctuation exchanges.

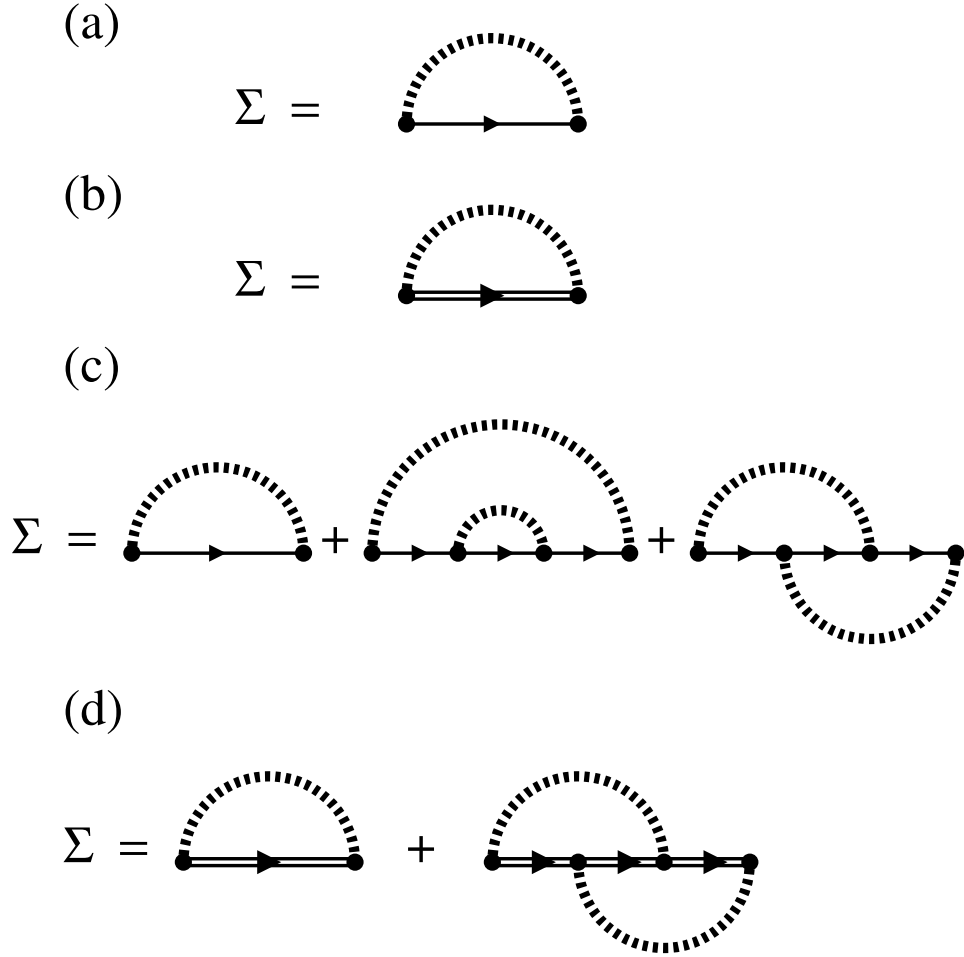
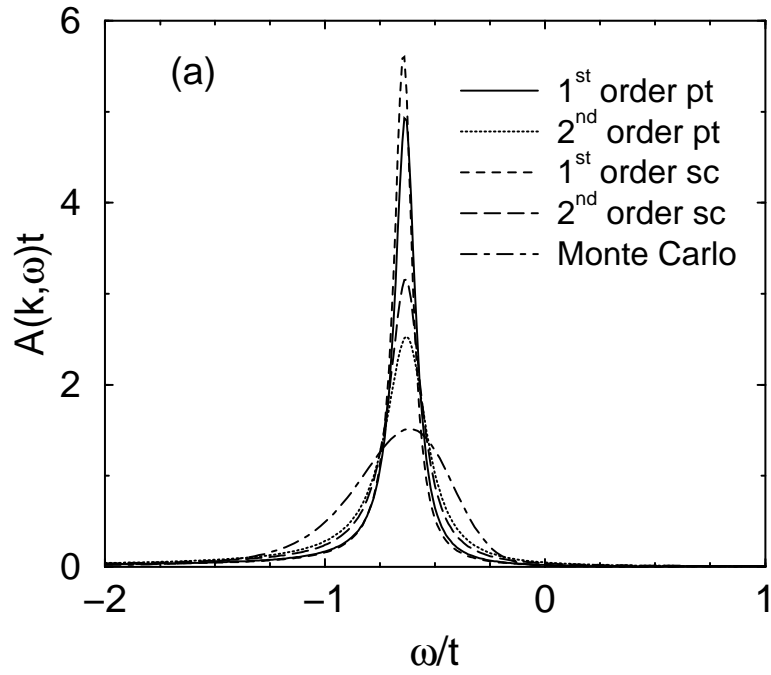
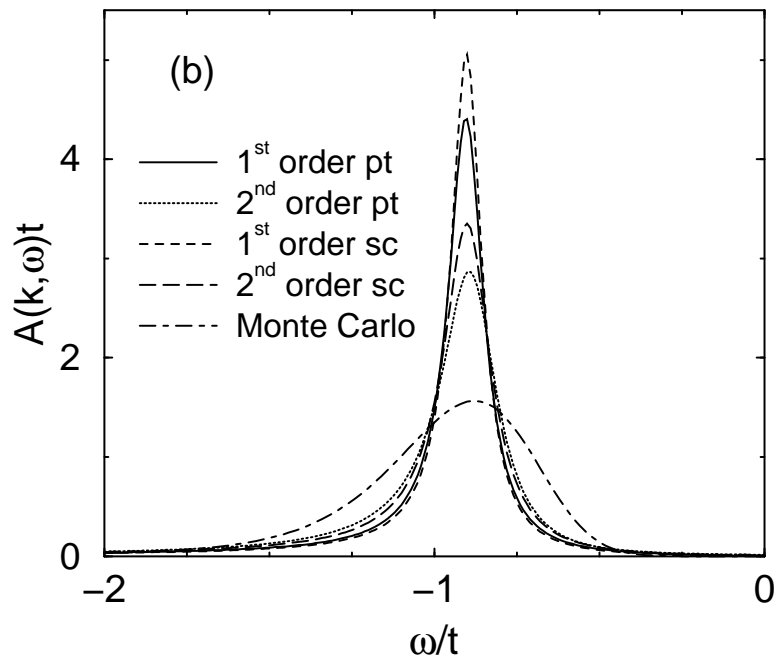


FIG. 2. The various perturbation-theoretic approximations to the quasiparticle self-energy considered in this paper. (a) First order perturbation theory. (b) First order self-consistent (Eliashberg). (c) Second order perturbation theory (d) Second order self-consistent. In this figure a single line denotes the bare quasiparticle propagator G_0 while a double line denotes the dressed propagator G to be determined self-consistently.

AF fluctuations ; $k = (\pi, 0)$; $\kappa^2 = 4.00$



AF fluctuations ; $k = (\pi/4, \pi/4)$; $\kappa^2 = 4.00$



AF fluctuations ; $\kappa^2 = 4.00$

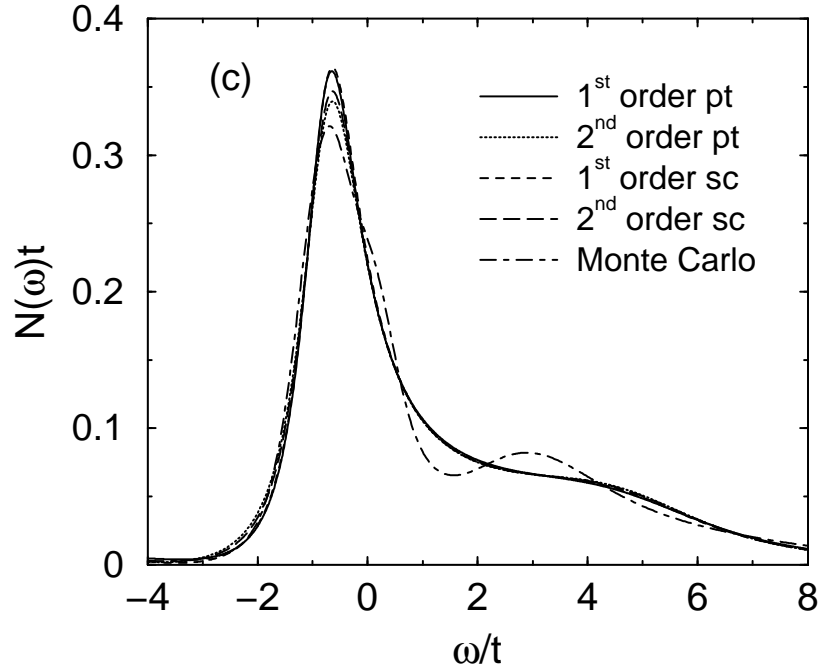
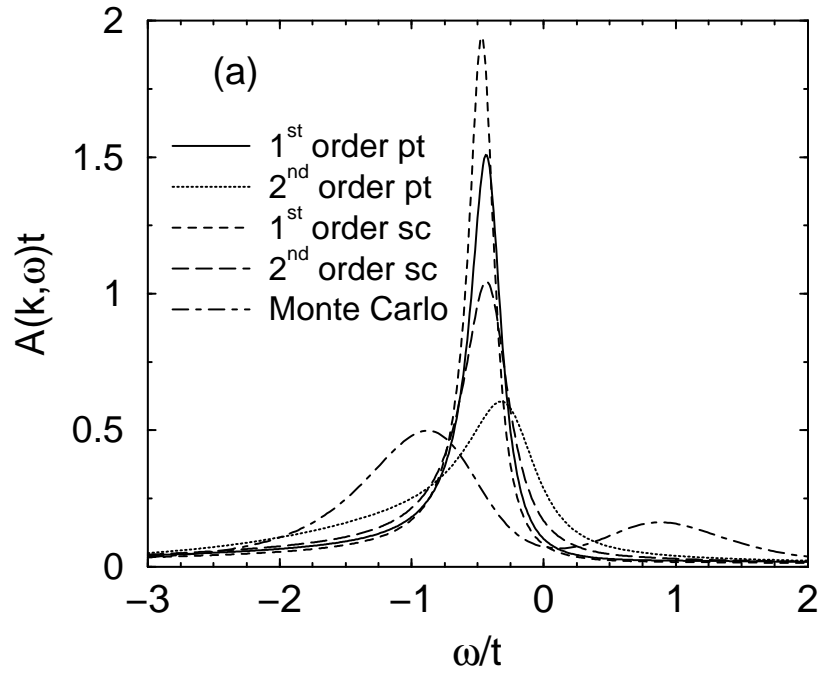
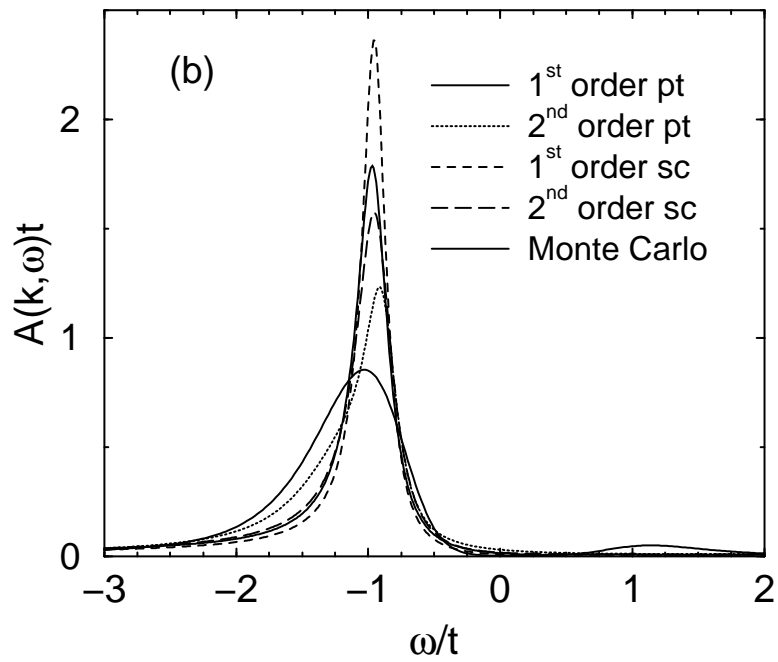


FIG. 3. The various perturbation-theoretic approximations to the spectral function $A(\mathbf{k}, \omega)$ and tunneling density of states $N(\omega)$ are compared to the results of the Monte Carlo simulations for $\kappa^2 = 4$ in the case of quasiparticles coupled to antiferromagnetic spin-fluctuations. 1st order pt corresponds to the approximation to the self-energy shown in Fig. 2a and given by Eq.(2.25). 2nd order pt corresponds to the approximation to the self-energy shown in Fig. 2c and given by Eq.(2.27). 1st order sc corresponds to the approximation to the self-energy shown in Fig. 2b and given by Eq.(2.26). 2nd order sc corresponds to the approximation to the self-energy shown in Fig. 2d and given by Eq.(2.28). (a) $A(\mathbf{k}, \omega)$ at $\mathbf{k} = (\pi, 0)$. (b) $A(\mathbf{k}, \omega)$ at $\mathbf{k} = (\pi/4, \pi/4)$. (c) $N(\omega)$.

AF fluctuations ; $k = (\pi, 0)$; $\kappa^2 = 1.00$



AF fluctuations ; $k = (\pi/4, \pi/4)$; $\kappa^2 = 1.00$



AF fluctuations ; $\kappa^2 = 1.00$

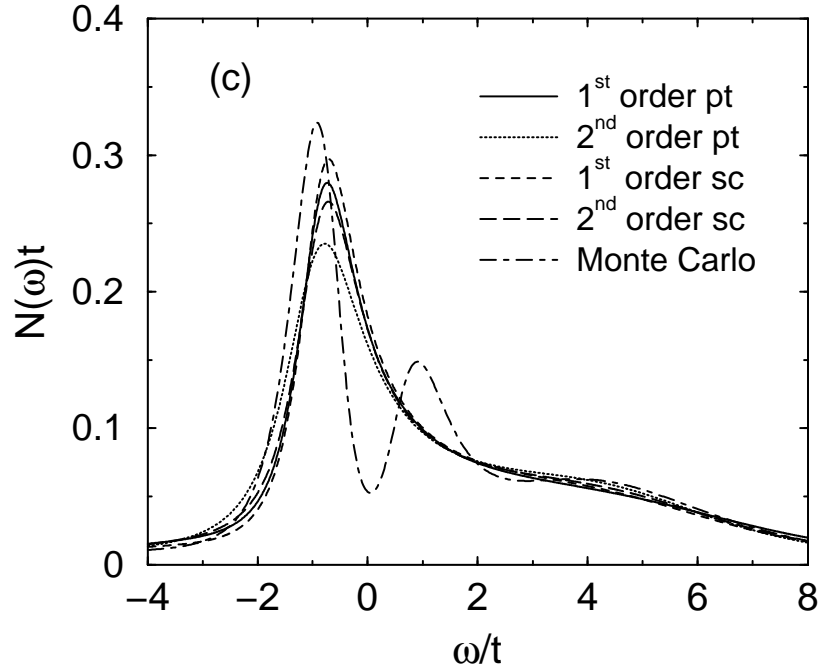
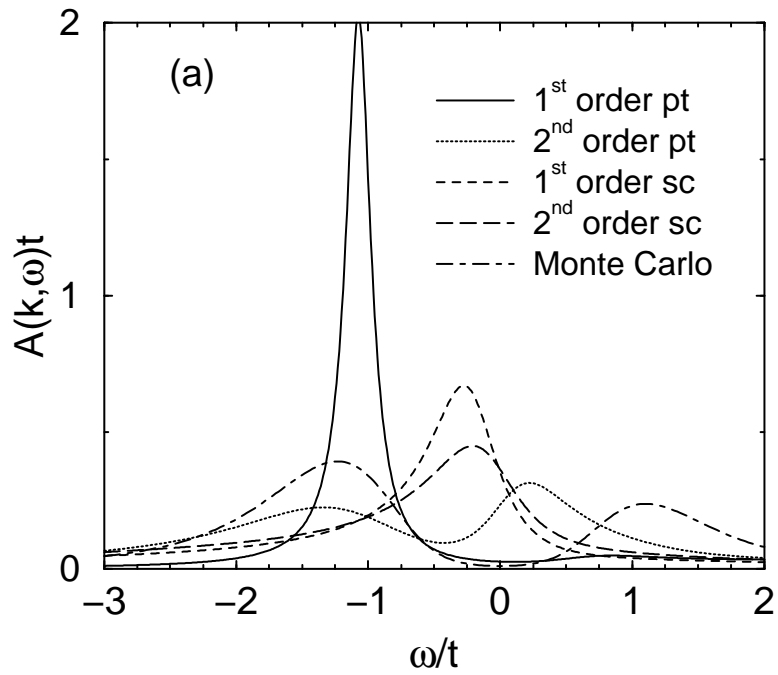
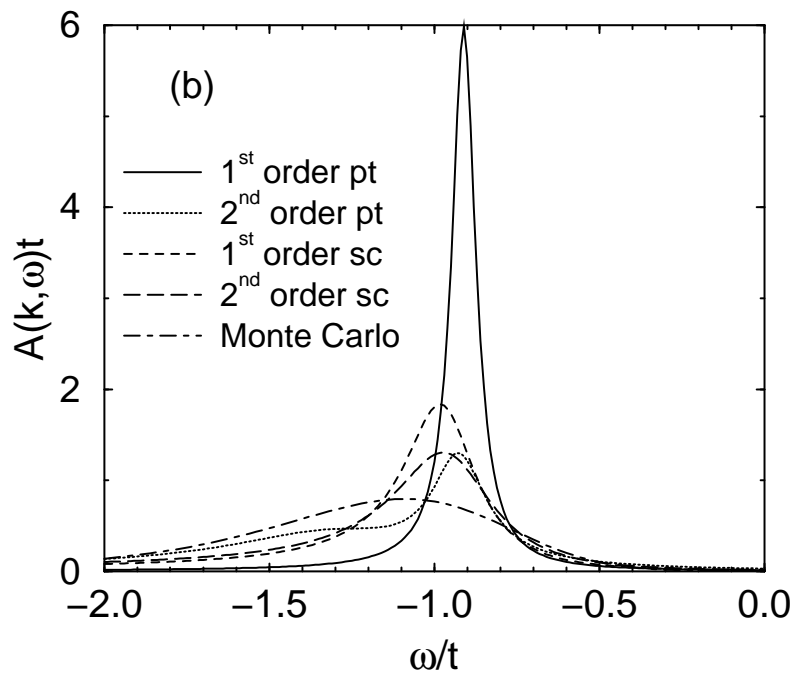


FIG. 4. The various perturbation-theoretic approximations to the spectral function $A(\mathbf{k}, \omega)$ and tunneling density of states $N(\omega)$ are compared to the results of the Monte Carlo simulations for $\kappa^2 = 1$ in the case of quasiparticles coupled to antiferromagnetic spin-fluctuations. 1st order pt corresponds to the approximation to the self-energy shown in Fig. 2a and given by Eq.(2.25). 2nd order pt corresponds to the approximation to the self-energy shown in Fig. 2c and given by Eq.(2.27). 1st order sc corresponds to the approximation to the self-energy shown in Fig. 2b and given by Eq.(2.26). 2nd order sc corresponds to the approximation to the self-energy shown in Fig. 2d and given by Eq.(2.28). (a) $A(\mathbf{k}, \omega)$ at $\mathbf{k} = (\pi, 0)$. (b) $A(\mathbf{k}, \omega)$ at $\mathbf{k} = (\pi/4, \pi/4)$. (c) $N(\omega)$.

AF fluctuations ; $k = (\pi, 0)$; $\kappa^2 = 0.25$



AF fluctuations ; $k = (\pi/4, \pi/4)$; $\kappa^2 = 0.25$



AF fluctuations ; $\kappa^2 = 0.25$

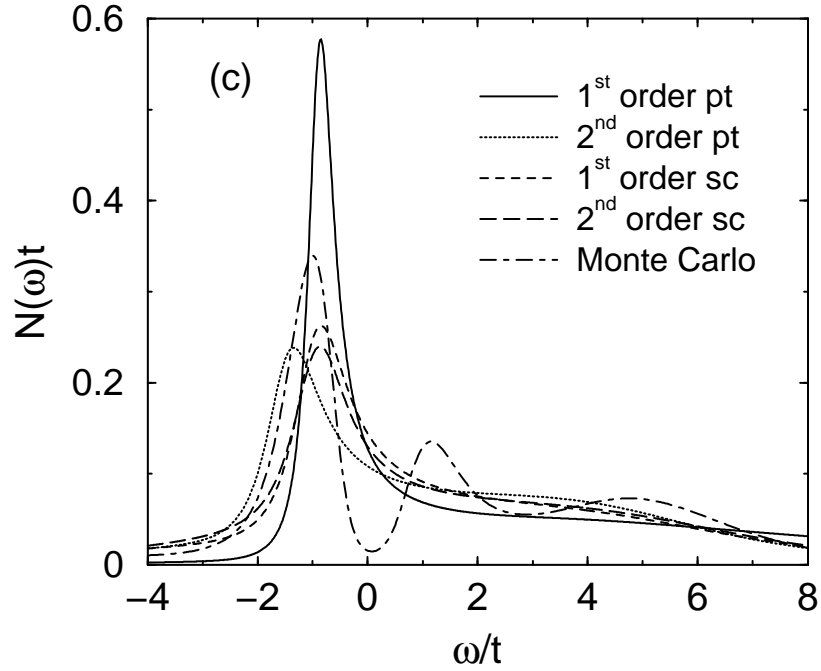
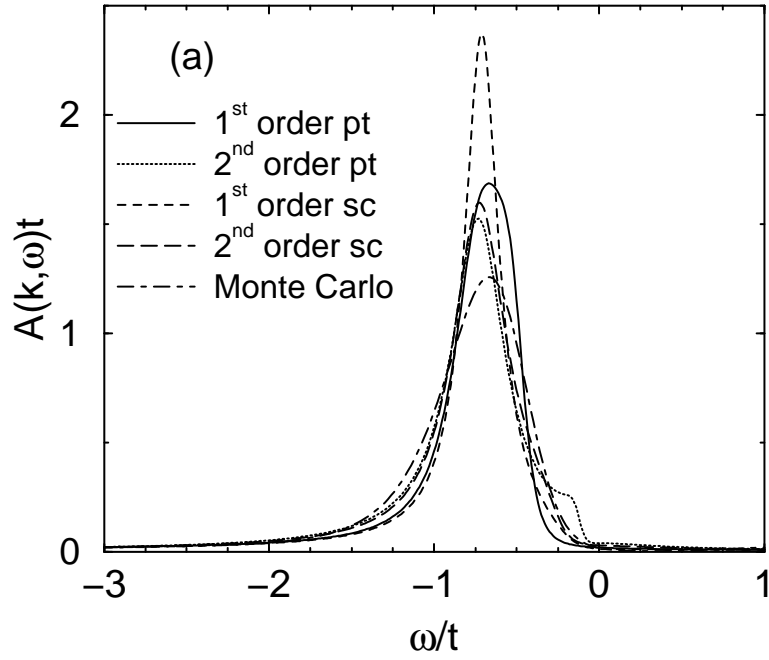
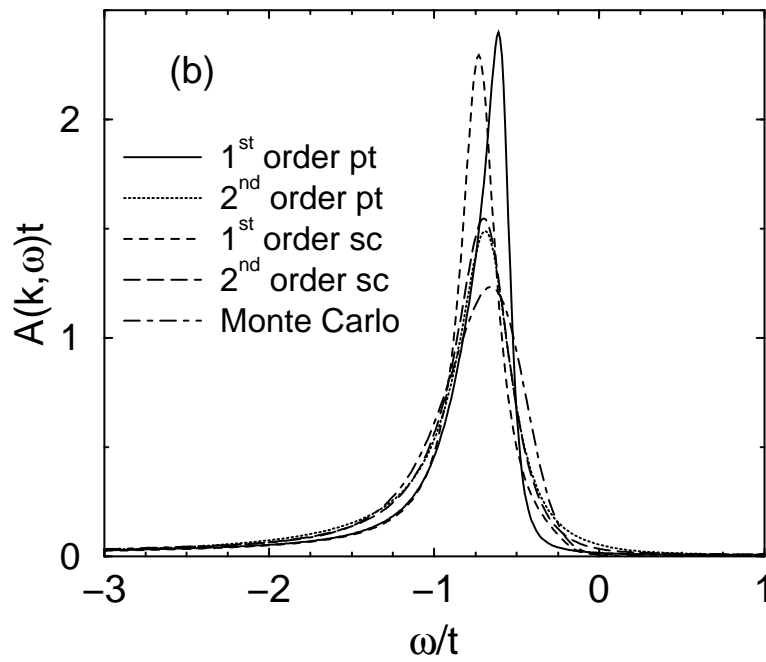


FIG. 5. The various perturbation-theoretic approximations to the spectral function $A(\mathbf{k}, \omega)$ and tunneling density of states $N(\omega)$ are compared to the results of the Monte Carlo simulations for $\kappa^2 = 0.25$ in the case of quasiparticles coupled to antiferromagnetic spin-fluctuations. 1st order pt corresponds to the approximation to the self-energy shown in Fig. 2a and given by Eq.(2.25). 2nd order pt corresponds to the approximation to the self-energy shown in Fig. 2c and given by Eq.(2.27). 1st order sc corresponds to the approximation to the self-energy shown in Fig. 2b and given by Eq.(2.26). 2nd order sc corresponds to the approximation to the self-energy shown in Fig. 2d and given by Eq.(2.28). (a) $A(\mathbf{k}, \omega)$ at $\mathbf{k} = (\pi, 0)$. (b) $A(\mathbf{k}, \omega)$ at $\mathbf{k} = (\pi/4, \pi/4)$. (c) $N(\omega)$.

FE fluctuations ; $k = (\pi, 0)$; $\kappa^2 = 4.00$



FE fluctuations ; $k = (\pi/4, \pi/4)$; $\kappa^2 = 4.00$



FE fluctuations ; $\kappa^2 = 4.00$

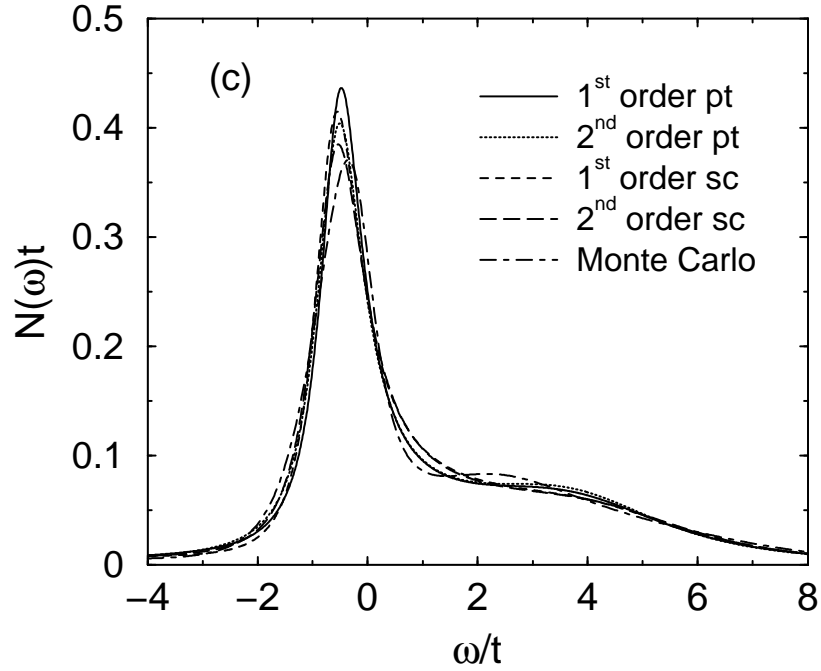
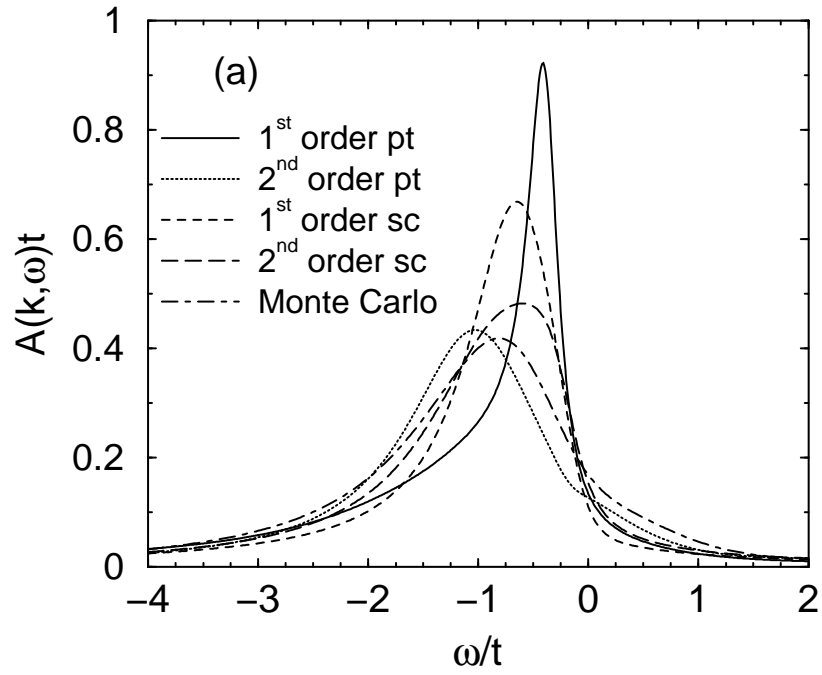
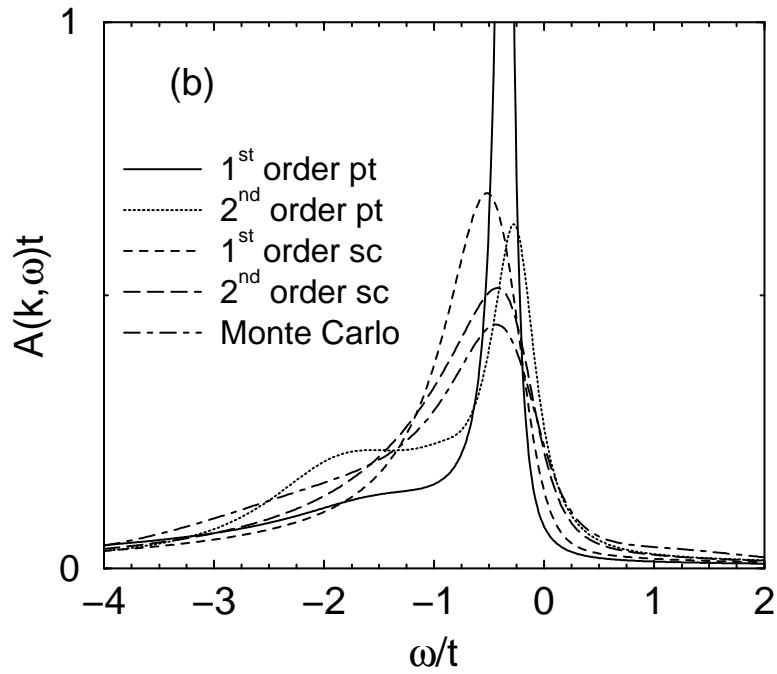


FIG. 6. The various perturbation-theoretic approximations to the spectral function $A(\mathbf{k}, \omega)$ and tunneling density of states $N(\omega)$ are compared to the results of the Monte Carlo simulations for $\kappa^2 = 4$ in the case of quasiparticles coupled to ferromagnetic spin-fluctuations. 1^{st} order pt corresponds to the approximation to the self-energy shown in Fig. 2a and given by Eq.(2.25). 2^{nd} order pt corresponds to the approximation to the self-energy shown in Fig. 2c and given by Eq.(2.27). 1^{st} order sc corresponds to the approximation to the self-energy shown in Fig. 2b and given by Eq.(2.26). 2^{nd} order sc corresponds to the approximation to the self-energy shown in Fig. 2d and given by Eq.(2.28). (a) $A(\mathbf{k}, \omega)$ at $\mathbf{k} = (\pi, 0)$. (b) $A(\mathbf{k}, \omega)$ at $\mathbf{k} = (\pi/4, \pi/4)$. (c) $N(\omega)$.

FE fluctuations ; $k = (\pi, 0)$; $\kappa^2 = 1.00$



FE fluctuations ; $k = (\pi/4, \pi/4)$; $\kappa^2 = 1.00$



FE fluctuations ; $\kappa^2 = 1.00$

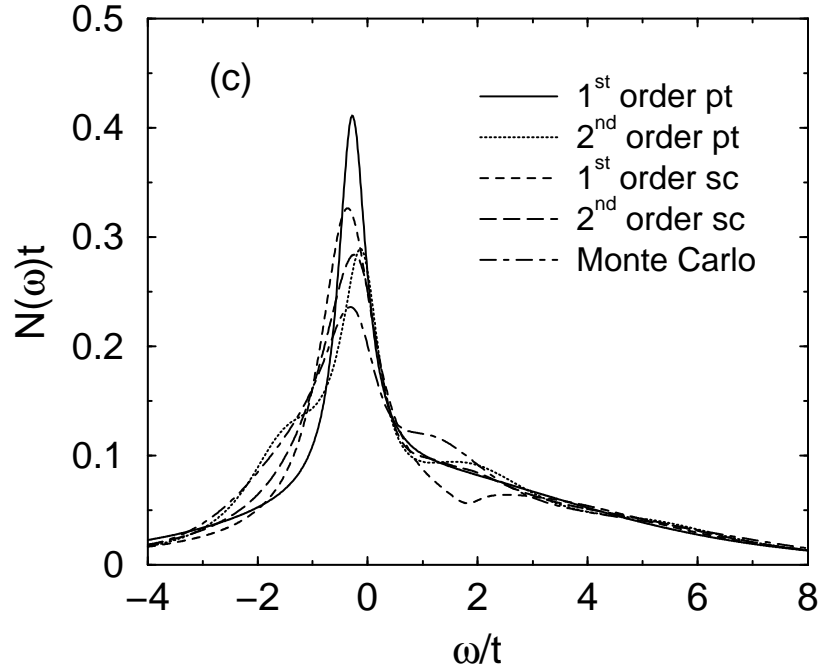
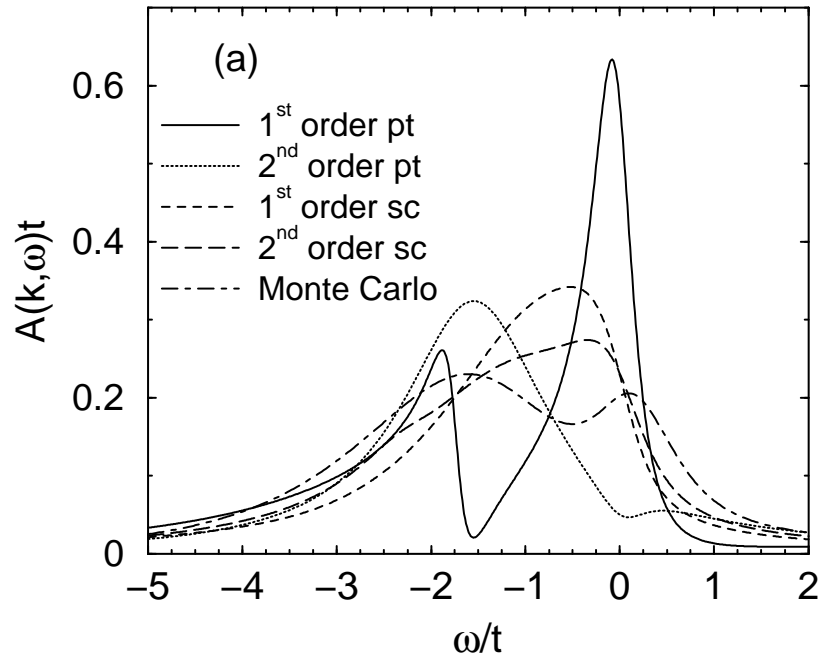
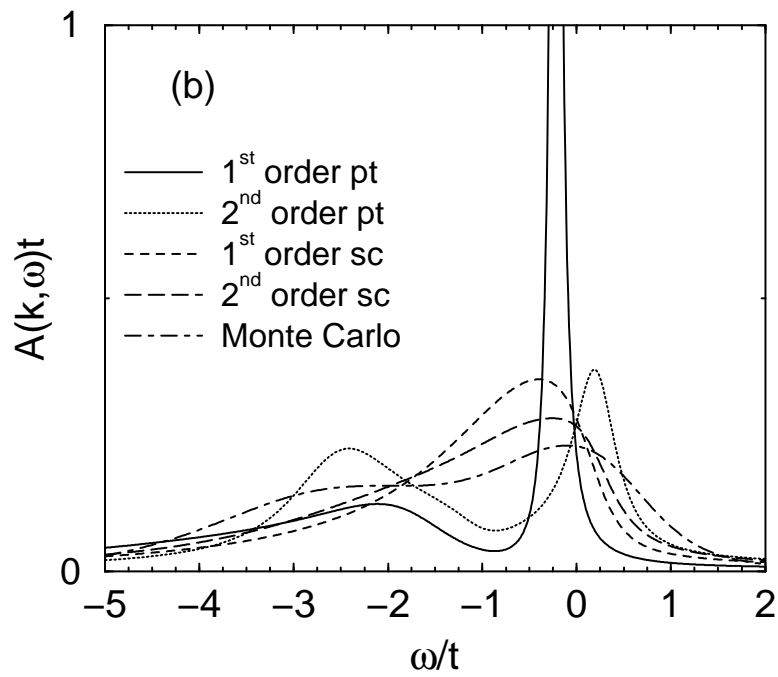


FIG. 7. The various perturbation-theoretic approximations to the spectral function $A(\mathbf{k}, \omega)$ and tunneling density of states $N(\omega)$ are compared to the results of the Monte Carlo simulations for $\kappa^2 = 1$ in the case of quasiparticles coupled to ferromagnetic spin-fluctuations. 1^{st} order pt corresponds to the approximation to the self-energy shown in Fig. 2a and given by Eq.(2.25). 2^{nd} order pt corresponds to the approximation to the self-energy shown in Fig. 2c and given by Eq.(2.27). 1^{st} order sc corresponds to the approximation to the self-energy shown in Fig. 2b and given by Eq.(2.26). 2^{nd} order sc corresponds to the approximation to the self-energy shown in Fig. 2d and given by Eq.(2.28). (a) $A(\mathbf{k}, \omega)$ at $\mathbf{k} = (\pi, 0)$. (b) $A(\mathbf{k}, \omega)$ at $\mathbf{k} = (\pi/4, \pi/4)$. (c) $N(\omega)$.

FE fluctuations ; $k = (\pi, 0)$; $\kappa^2 = 0.25$



FE fluctuations ; $k = (\pi/4, \pi/4)$; $\kappa^2 = 0.25$



FE fluctuations ; $\kappa^2 = 0.25$

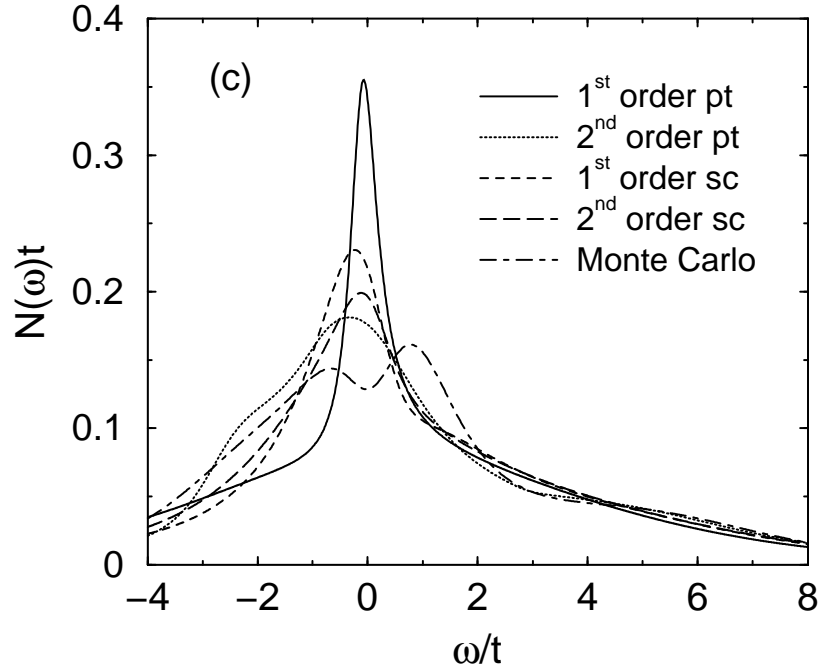
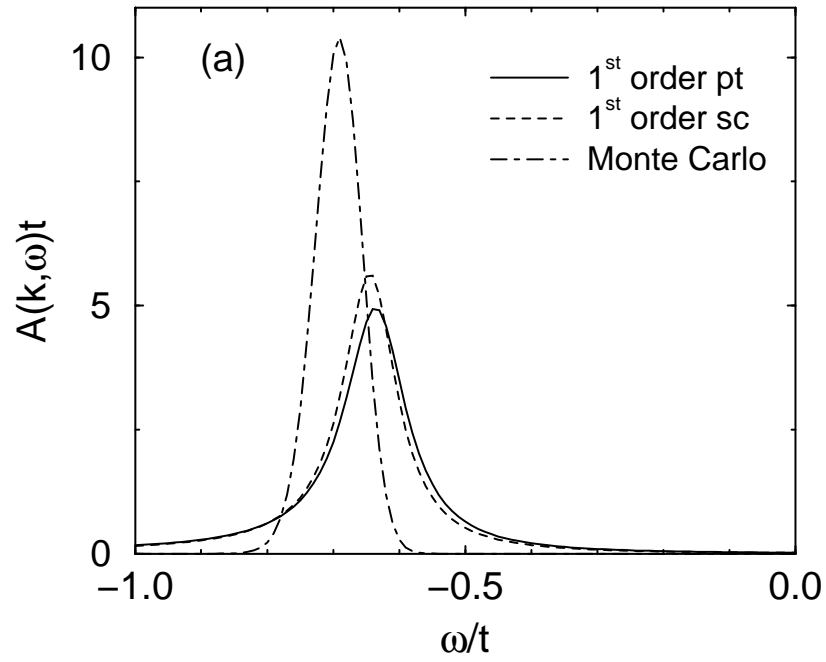
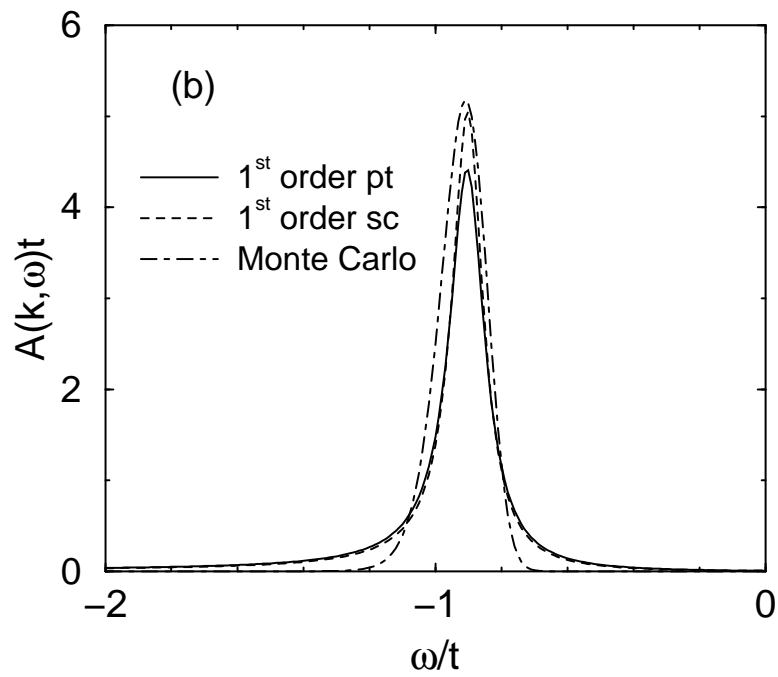


FIG. 8. The various perturbation-theoretic approximations to the spectral function $A(\mathbf{k}, \omega)$ and tunneling density of states $N(\omega)$ are compared to the results of the Monte Carlo simulations for $\kappa^2 = 0.25$ in the case of quasiparticles coupled to ferromagnetic spin-fluctuations. 1st order pt corresponds to the approximation to the self-energy shown in Fig. 2a and given by Eq.(2.25). 2nd order pt corresponds to the approximation to the self-energy shown in Fig. 2c and given by Eq.(2.27). 1st order sc corresponds to the approximation to the self-energy shown in Fig. 2b and given by Eq.(2.26). 2nd order sc corresponds to the approximation to the self-energy shown in Fig. 2d and given by Eq.(2.28). (a) $A(\mathbf{k}, \omega)$ at $\mathbf{k} = (\pi, 0)$. (b) $A(\mathbf{k}, \omega)$ at $\mathbf{k} = (\pi/4, \pi/4)$. (c) $N(\omega)$.

Charge fluctuations ; $k = (\pi, 0)$; $\kappa^2 = 4.00$



Charge fluctuations ; $k = (\pi/4, \pi/4)$; $\kappa^2 = 4.00$



Charge fluctuations ; $\kappa^2 = 4.00$

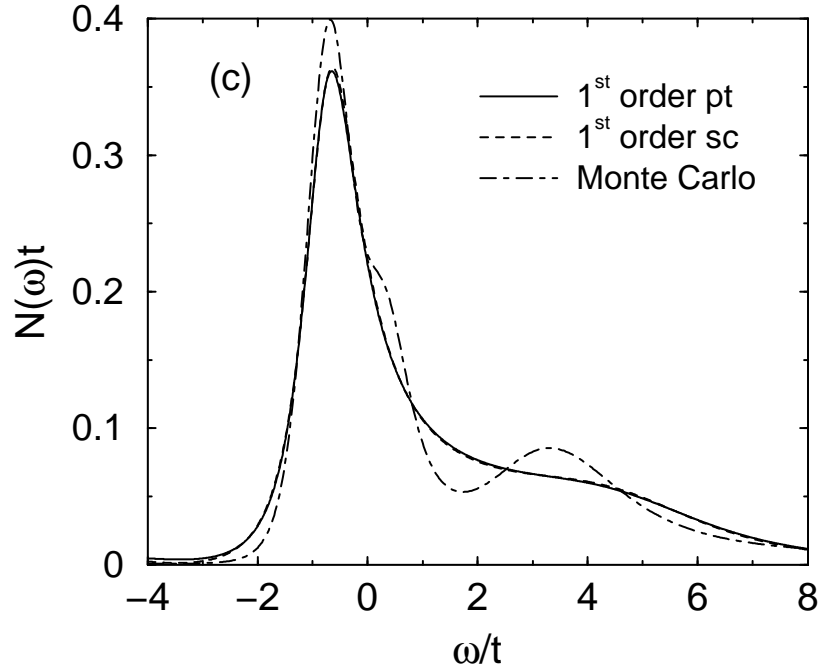
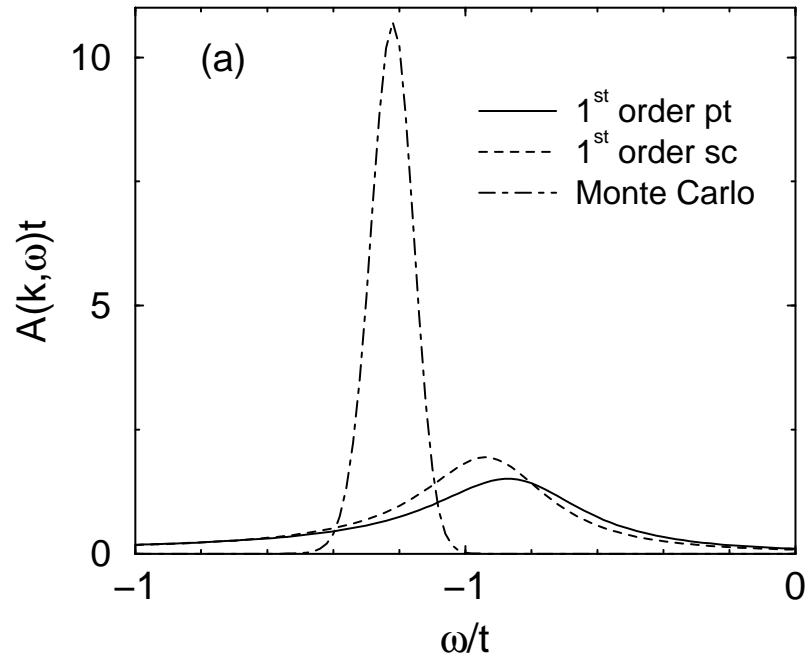
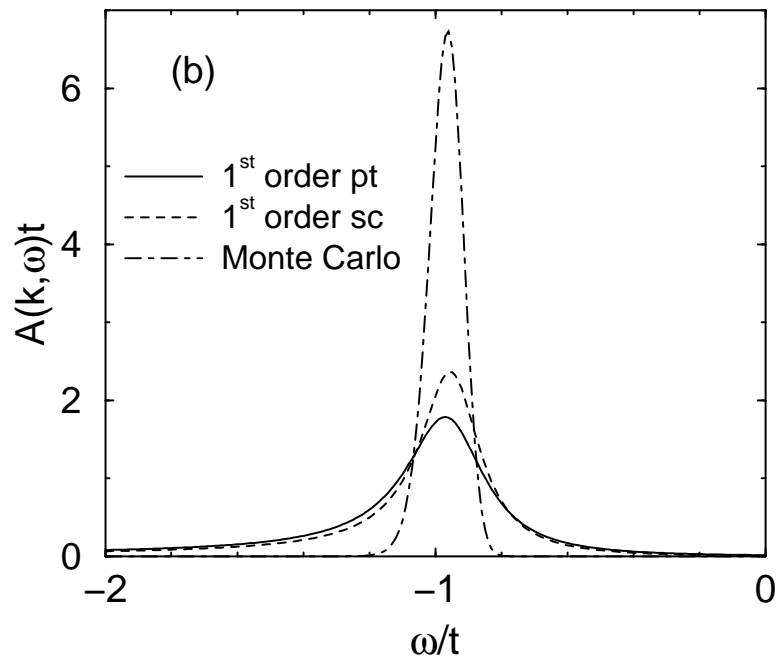


FIG. 9. The various perturbation-theoretic approximations to the spectral function $A(\mathbf{k}, \omega)$ and tunneling density of states $N(\omega)$ are compared to the results of the Monte Carlo simulations for $\kappa^2 = 4$ in the case of quasiparticles coupled to charge fluctuations. 1^{st} order pt corresponds to the approximation to the self-energy shown in Fig. 2a and given by Eq.(2.25). 1^{st} order sc corresponds to the approximation to the self-energy shown in Fig. 2b and given by Eq.(2.26). (a) $A(\mathbf{k}, \omega)$ at $\mathbf{k} = (\pi, 0)$. (b) $A(\mathbf{k}, \omega)$ at $\mathbf{k} = (\pi/4, \pi/4)$. (c) $N(\omega)$.

Charge fluctuations ; $k = (\pi, 0)$; $\kappa^2 = 1.00$



Charge fluctuations ; $k = (\pi/4, \pi/4)$; $\kappa^2 = 1.00$



Charge fluctuations ; $\kappa^2 = 1.00$

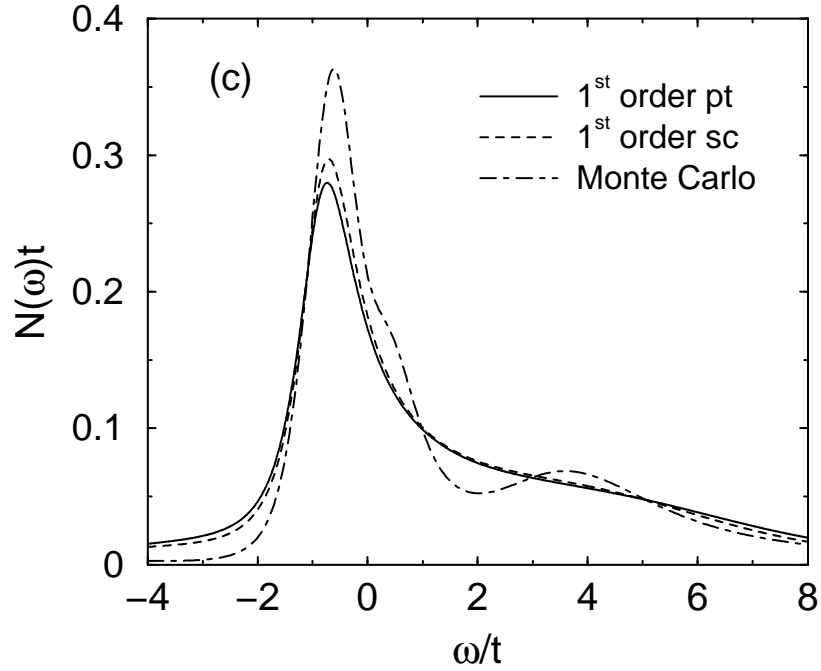
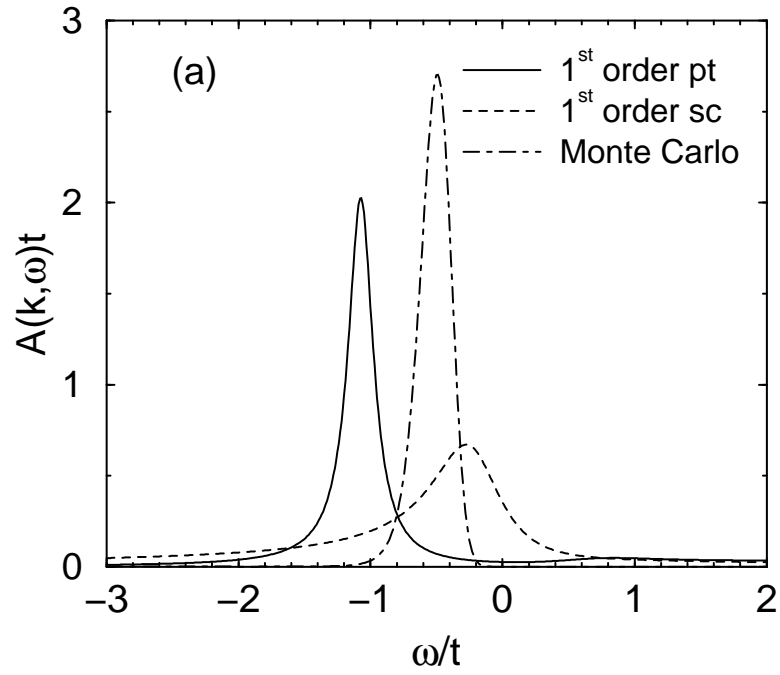
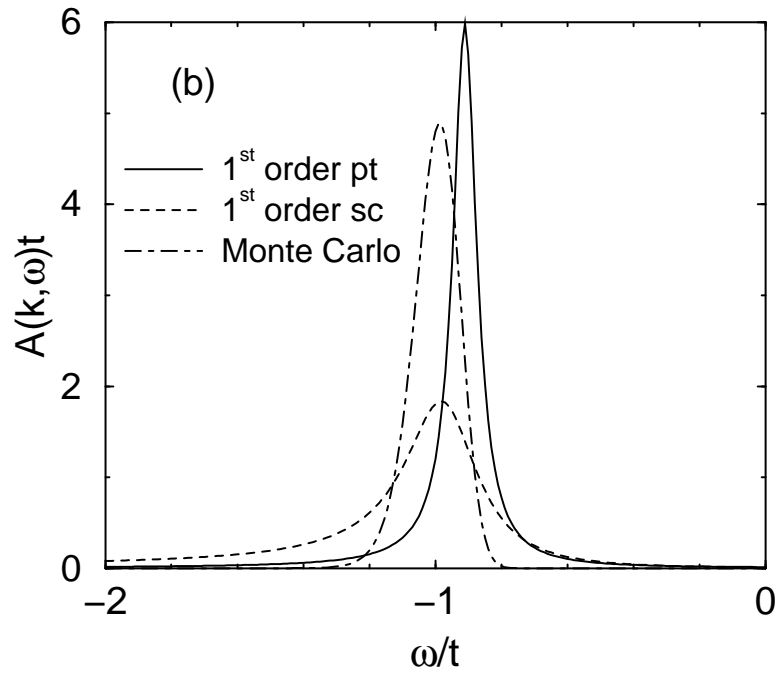


FIG. 10. The various perturbation-theoretic approximations to the spectral function $A(\mathbf{k}, \omega)$ and tunneling density of states $N(\omega)$ are compared to the results of the Monte Carlo simulations for $\kappa^2 = 1$ in the case of quasiparticles coupled to charge fluctuations. 1^{st} order pt corresponds to the approximation to the self-energy shown in Fig. 2a and given by Eq.(2.25). 1^{st} order sc corresponds to the approximation to the self-energy shown in Fig. 2b and given by Eq.(2.26). (a) $A(\mathbf{k}, \omega)$ at $\mathbf{k} = (\pi, 0)$. (b) $A(\mathbf{k}, \omega)$ at $\mathbf{k} = (\pi/4, \pi/4)$. (c) $N(\omega)$.

Charge fluctuations ; $k = (\pi, 0)$; $\kappa^2 = 0.25$



Charge fluctuations ; $k = (\pi/4, \pi/4)$; $\kappa^2 = 0.25$



Charge fluctuations ; $\kappa^2 = 0.25$

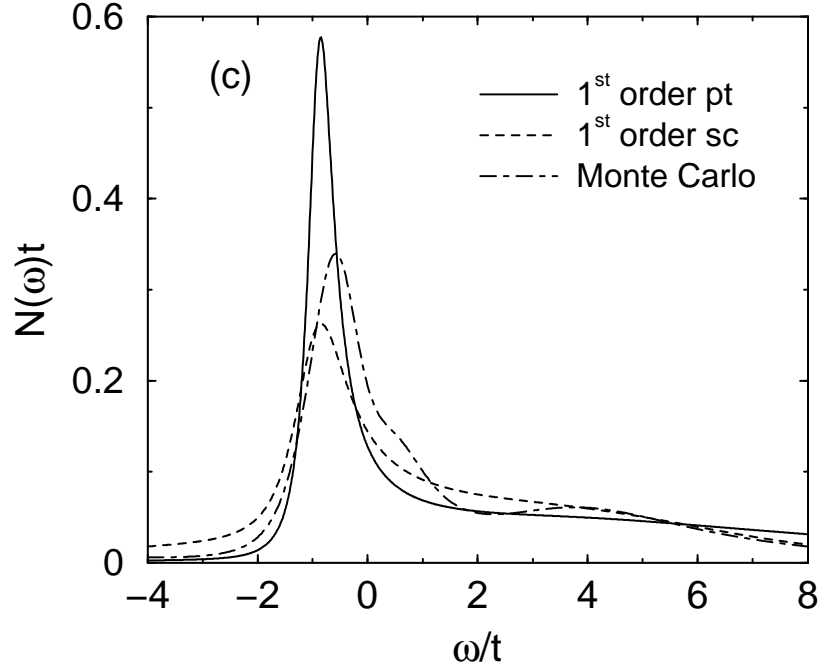


FIG. 11. The various perturbation-theoretic approximations to the spectral function $A(\mathbf{k}, \omega)$ and tunneling density of states $N(\omega)$ are compared to the results of the Monte Carlo simulations for $\kappa^2 = 0.25$ in the case of quasiparticles coupled to charge fluctuations. 1st order pt corresponds to the approximation to the self-energy shown in Fig. 2a and given by Eq.(2.25). 1st order sc corresponds to the approximation to the self-energy shown in Fig. 2b and given by Eq.(2.26). (a) $A(\mathbf{k}, \omega)$ at $\mathbf{k} = (\pi, 0)$. (b) $A(\mathbf{k}, \omega)$ at $\mathbf{k} = (\pi/4, \pi/4)$. (c) $N(\omega)$.